Received February 1, 2017

SALINITY AND SALINITY RESPONSE IN SAN ANTONIO BAY

George H. Ward, Ph.D.
Center for Research in Water Resources
The University of Texas at Austin

TWDB – UTA Interagency Contract No. 1300011546
TWDB – TGLO Interagency Contract No. 1300011545 and 13-150-000-7240
USFWS Contract No. F12AF01002
Biological Study of San Antonio Bay

Project Officer: Carla Guthrie, Ph.D.
Ssurface Water Resources Division
Texas Water Development Board

31 December 2013

THIS REPORT (STUDY) IS FUNDED WITH QUALIFIED OUTER CONTINENTAL SHELF OIL AND GAS REVENUES BY THE COASTAL IMPACT ASSISTANCE PROGRAM, U.S. FISH AND WILDLIFE SERVICE, U.S. DEPARTMENT OF THE INTERIOR. THE VIEWS AND CONCLUSIONS EXPRESSED HEREIN ARE THOSE OF THE AUTHOR(S) AND DO NOT NECESSARILY REFLECT THE VIEWS OF THE U.S. GOVERNMENT.

CONTENTS

FIGURES

FIGURES
(continued)

TABLES

1. SALINITY INTRUSION AND EXTRUSION IN AN ESTUARY

An estuary, by definition, is a coastal watercourse that is transitional between the terrestrial and marine environments. An estuary is therefore subject to external factors deriving from both the ocean and land, as well as some factors that are peculiar to the coastal zone. Among the oceanic influences are tides, waves, marine meteorology and seasonal water-level variation. Among the terrestrial influences are continental meteorology, sediment transport from erosion of the surface, and, most importantly, drainage of runoff, i.e. freshwater inflow, into the estuary. (See, e.g., Ward and Montague, 1996, for more detail on the estuarine environment.) Thus, either within or immediately adjacent to the boundary of an estuary, seawater is brought into juxtaposition with freshwater.

The most fundamental distinction between freshwater and seawater is the salt content or salinity, the concentration of dissolved salts measured as mass of salt per unit mass of water. The salinity of seawater is nominally 3.5%, or, in the more conventional units, 35‰, i.e., parts per thousand (often designated *ppt*; the modern equivalent is *psu*, "practical salinity units"). The salinity of freshwater is nominally zero (0). Both freshwater and seawater salinity exhibit small fluctuations about these values, which can be important for watermass differentiation in the ocean and associated dynamics, or in tracing loads of minerals or wastes in rivers, but are generally of little significance in an estuary (see, e.g., Mangelsdorf, 1967). Because of the dissolved salts, a volume of seawater will be heavier than a volume of freshwater by about 3%.

Where freshwater is brought into juxtaposition with seawater, several processes effect the intermixing of the two, resulting in a gradient zone in which salinity increases from zero at its inland freshwater limit to oceanic salinity. Figure 1 shows a simple idealized estuary with schematic salinity contours ("isohalines"). Generally, for higher river flows, the salinity gradient zone is displaced farther down the estuary and oceanic salinities are reached farther out in the nearshore zone. For lower river flows, in contrast, the salinity gradient retreats farther up the estuary. For very low flows, oceanic salinities may be found well within the estuary bounds.

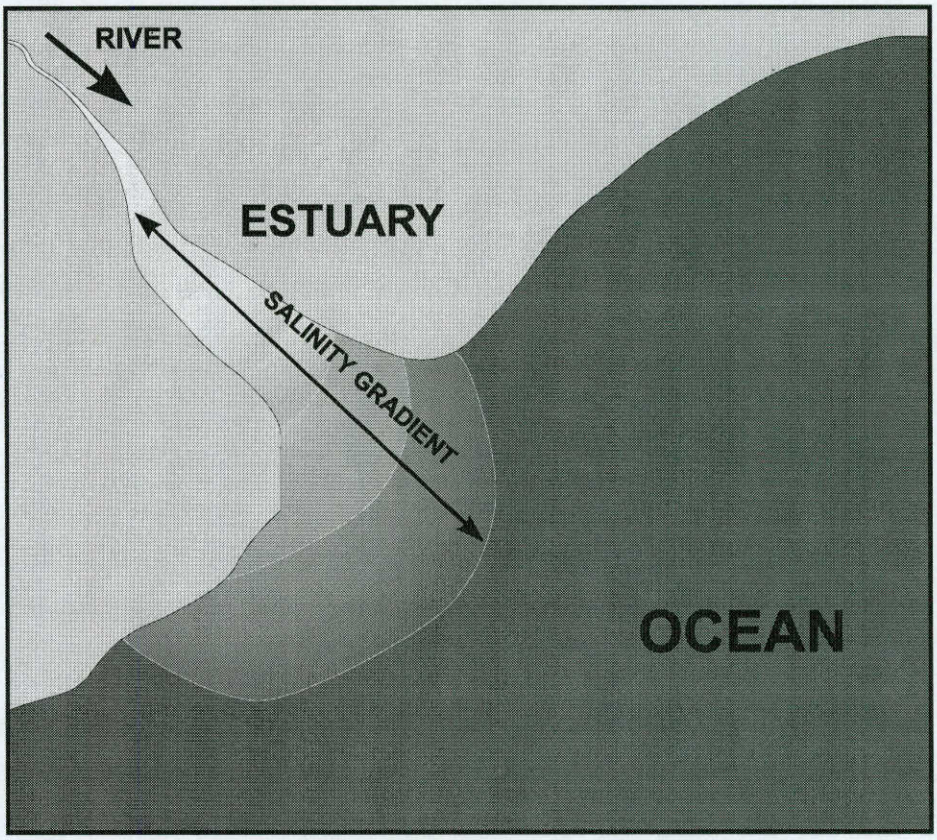

Figure 1 - Schematic of simple estuary, showing salinity gradient from fresh to oceanic

Most estuaries are much more complex than the idealization of Fig. 1. The physiography and bathymetry of the estuary may be highly varied, with deep channels and extensive shoals, there may be multiple points of freshwater flow entry, and the connection to the sea may be obstructed by sills, reefs or islands. The bays of Texas are estuaries of a type known as lagoonal or bar-built (Ward and Montague, 1996). These are broad, relatively shallow systems fronted by a barrier island. Exchange with the sea occurs through narrow tidal inlets through the barrier island.

Estuaries have salinities less than oceanic due to dilution by freshwater inflow. This would lead one to expect salinity at a point in an estuary to be a nicely behaved, monotonically decreasing

function of inflow. Conceptually, a specific value of inflow implies a specific corresponding value of salinity: the higher the inflow the lower the salinity, and *vice versa.* Actual data from estuaries belie this expectation however, exhibiting considerable scatter on a graph of salinity plotted versus inflow. ("Buckshot" is an apt description.) This scatter is due largely to the complexity of the response of salinity to inflow. An example of how this scatter arises is the response of salinity to a varying influx of freshwater.

A relatively slow influx of freshwater can be mixed into the water in the estuary by natural turbulence. If this influx increases to a substantial flow, it begins to displace, rather than mix into, the water resident in the estuary. A flood hydrograph can replace much, sometimes all, of the volume of the estuary. This is an example of salinity *extrusion*, which refers to any hydrodynamic process that transports water from the estuary into the ocean, in the process reducing the salinity in the estuary. Freshwater inflow is the most prominent such extrusion process, but removal of water from the estuary volume by tides, wind stress, or large-scale water movement in the coastal ocean also accomplish salinity extrusion.

As this freshwater influx displaces the estuary water, the salinity at a fixed location in the estuary drops to much lower, perhaps near-zero values. Saltier water from the ocean then begins working back into the estuary, transported by tides, turbulent mixing, and the greater density of saltwater, so that salinity begins to rise. These processes are referred to collectively as salinity *intrusion.* The result of freshwater displacement followed by salinity intrusion means that the time behavior of salinity is different from that of the freshwater inflow: salinity exhibits a lagged, integrated response to the excitation of the inflow time function.

A schematic example is shown in Figure 2, which might typify the idealized estuary of Fig. 1. Salinity at a fixed location in the estuary begins to drop after the rising limb of the flow hydrograph (how soon after depending upon the measurement location in the estuary), and decreases down to a low value determined by the diminishing but still substantial rate of inflow. As flow continues to decline, salinity begins to slowly increase due to intrusion and mixing. For most of the values of flow, there are two occurrences on this graph, one on the rising limb and

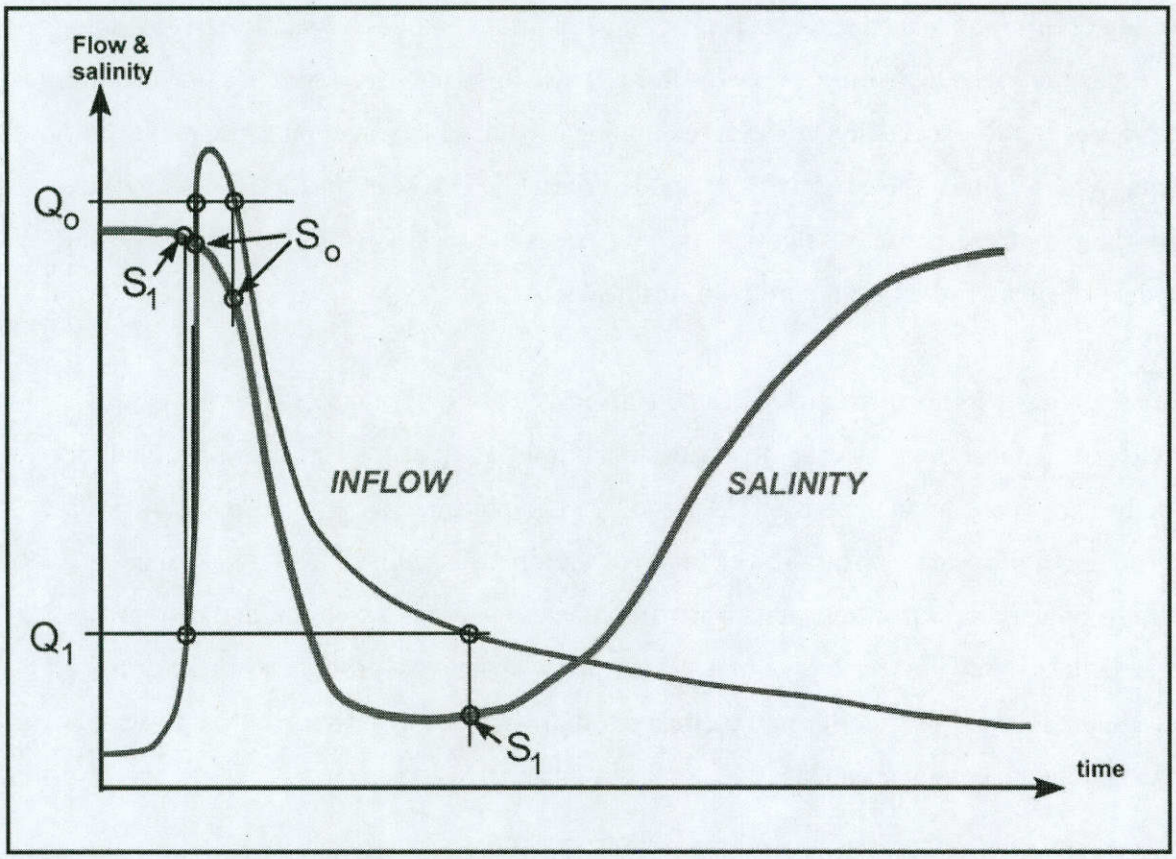

Figure 2 - Schematic of salinity response to a single flood hydrograph

one on the falling limb of the hydrograph. In Fig. 2, for example, the two values of each of Q_o and Q_1 (a high flow and a low flow) and marked on the flow hydrograph. The two salinity values corresponding to these two occurrences of the *same* flow value are generally different, exemplified by the two values of S_o corresponding to Q_o and two values of S_1 corresponding to Q_1. These may differ widely, such as the example of S_1 in Fig. 2. If this time plot were sampled at intervals of time (as one would do if making routine measurements of salinity at a fixed location in the estuary) and the results plotted as salinity versus inflow, there would result considerable scatter because of the different salinity values for each value of inflow.

Table 1
Principal astronomical harmonics forcing the ocean tide, see Pugh (1987)

name	*frequency designation*	*period**	
solar day	σ_0	24	hours
lunar day	σ_1	24.84	hours
tropical month	σ_3	27.32	days
tropical year	σ_4	365.24	days
lunar perigee rotation	σ_5	8.85	years
lunar nodal retrogression	σ_6	18.6	years

*mean solar time

In the real world, neat isolated hydrographs like that of Fig. 2 rarely occur. Instead, there are multiple, superposed hydrographs forming a complex time series in which both flow and salinity exhibit an even more complex response, giving multiple values of salinity for a specific value of inflow. Moreover, salinity also responds to other processes that have no direct relation to inflow, which further contribute to the scatter. These processes include circulations internal to the estuary driven by wind and tidal currents, direct precipitation, and evaporation from the water surface.

Salinity intrusion processes transport ocean water into the estuary, and operate in conjunction with turbulence to mix this higher salinity water with the estuary water. There are three such processes that are of central importance for salinity intrusion in most estuaries. The first is the astronomical tides, driven by the gravitational effects of the sun and moon on the ocean and therefore periodic. The most important astronomical frequencies are listed in Table 1. The water-level variation resulting from these effects can be decomposed into a sum of harmonics:

$$\zeta = \sum H_i \cos(f_i t - \varphi_i)$$

Table 2
Predominant components of the equilibrium tide, see Pugh (1987)

semidiurnal			*diurnal*		
designation	*frequency (degrees/hour)*	*period (hours)*	*designation*	*frequency (degrees/hour)*	*period (hours)*
M_2	28.984	12.42	K_1	15.041	23.93
S_2	30.000	12.00	O_1	13.943	25.82
N_2	28.440	12.66	P_1	14.959	24.07
K_2	30.082	11.97	Q_1	13.399	26.87

in which the frequencies f_i derive from orbital parameters of the sun-moon-earth system, including those in Table 1, plus their sums and differences. Theoretically, there are hundreds of such harmonics (referred to as *constituents* or *partials*). In practice, however, those considered are limited by the trade-off between computational effort and improvement in accuracy, as well as data availability. Most mechanical tide predictors used 20-40 constituents (Cartwright, 1999); Doodson (1928) addresses 61 constituents. In the open ocean, the harmonics mainly cluster in the semidiurnal band, about 12 hours, the diurnal band, about 24 hours, and longer periods, notably fortnightly. The four largest components in the first two clusters (called *species*) are given in Table 12-2. These include both solar and lunar days and half days.

In estuaries, tidal variation is forced by the tide at the estuary mouth, rather than by direct astronomical forcing within the estuary. Propagating into the estuary, the tide is further transformed by shallow depths and constrained physiography. Following Ward and Montague (1996), the behavior of tides in estuaries includes these properties:

- Each component of the tide, with period T, propagates as a long, shallow-water wave with speed (celerity) C, i.e. one whose wavelength $\lambda = CT$ is large compared to the mean water depth D.
- The celerity of the propagating wave is approximately $C = (gD)^{1/2}$, g denoting acceleration of gravity.

- In the open ocean, the tidal wave is progressive, that is, the water level and current are in phase.
- Friction is exerted as a quadratic stress, proportional to the square of current. The effects of friction are to dampen the amplitude of the tide and retard its propagation, and to stimulate higher harmonics (overtides) of the frequency $1/T$.
- The presence of barriers to flow, e.g., shorelines, dikes, bulkheads, locks and dams, allows wave reflection, so that the tide acquires additional components of period T propagating in directions opposite to the incoming wave. This creates a phase lag between water level and current. With distance up the estuary the tide is transformed from a progressive to a standing wave (water level and current 90° out of phase).
- In many estuaries with a diminishing cross section with distance upstream, there is a zone within this convergence of cross section in which the tidal amplitude increases, despite the attenuating effect of friction.
- While the tidal current is directed up and down the axis of a longitudinal estuary, broader systems, such as lagoons and tectonobays, allow the development of rotary currents, in which the direction of the tidal current varies through the full 360° with the turn of the tide.

A useful indicator of the relative effect of tides in an estuary is the volume of water brought into the estuary on the incoming tide, referred to as the tidal *prism*, compared to the estuary volume.

The second process bringing seawater into the estuary is similar to the tide in that it also involves a volume of water forced into the estuary from the ocean, but the forcing is directly or indirectly due to wind stress on the ocean surface. Like the tide, an increase of water level in the estuary is created, sometimes referred to as a "wind tide." The principal distinction is that, unlike astronomical tides, wind tides are aperiodic and therefore intrinsically unpredictable. The direct effect of wind stress is to drive a surface current in the direction of the wind. Onshore winds therefore drive surface waters into an estuary, in the process raising the elevation of the water surface. An example of indirect forcing by wind occurs in the presence of a barrier to this direct wind-driven flow, such as a groin, dike or barrier island. Because the wind exerts a stress both landward and seaward from this barrier, a differential in water level between the nearshore ocean and the water behind the barrier may be created that drives a flow flanking the barrier, such as through the inlet into the estuary. Another indirect response to wind stress is Ekman transport, in which the effect of the earth's rotation is to rotate the wind-driven current clockwise (in the northern hemisphere) from the direction of the wind. If the wind is directed parallel to the coast

with the coastline to the right of the wind, Ekman transport can lead to an accumulation of water in the nearshore that in turn drives an influx into the mouth of an estuary.

The third process bringing seawater into the estuary is the estuary density current, which arises from the horizontal gradient in salinity created by the mixing of freshwater and seawater. This type of circulation is peculiar to the estuary, and where it operates, can be the primary mechanism for salinity intrusion. The density current is driven by the *horizontal* gradient in density, and is therefore linked to the location and steepness of the estuary salinity gradient. It is unrelated to salinity stratification, and can operate in vertically well-mixed estuaries. In estuaries with a longitudinal geometry, such as a coastal-plain or river-channel estuary, the density current is manifested as a circulation in the longitudinal-vertical plane, with transport upstream in the lower layer of the estuary compensated by a seaward transport in the upper layer. The intensity of the circulation varies as the *cube* of water depth. This is why a dredged channel exerts such an effect of increasing the salinity of the estuary, despite its small proportion of the total volume of the estuary. More details on the mechanics of the estuary density current are given by Ward and Montague (1996) and references therein.

There are basically two strategies available to the analyst to establish the response of salinity in an estuary to freshwater inflow. The first is address the relation statistically, seeking a single-valued relation between salinity and inflow, accepting that the various processes summarized above will contribute scatter about any such relation. Estimating the magnitudes of the processes that accomplish salinity intrusion can, in some cases, help clarify the variance of salinity about the statistical relation. The second is to examine the time response of salinity to the time signal of freshwater inflow, separating the extrusion part of the response from the intrusion part associated with the recession of the hydrograph. Both strategies are applied to San Antonio Bay.

2. SALINITY DYNAMICS IN SAN ANTONIO BAY

2.1 Physiography and bathymetry of San Antonio Bay

A portion of the coastal bend of Texas is shown in Figure 3, in which San Antonio Bay is indicated. From a large-scale viewpoint, Corpus Christi Bay, Aransas-Copano Bay, San Antonio Bay and Matagorda Bay can, together, be considered a single estuarine system, with multiple river inflows and with two primary inlets for exchange with the sea, *viz*. Aransas Pass on the

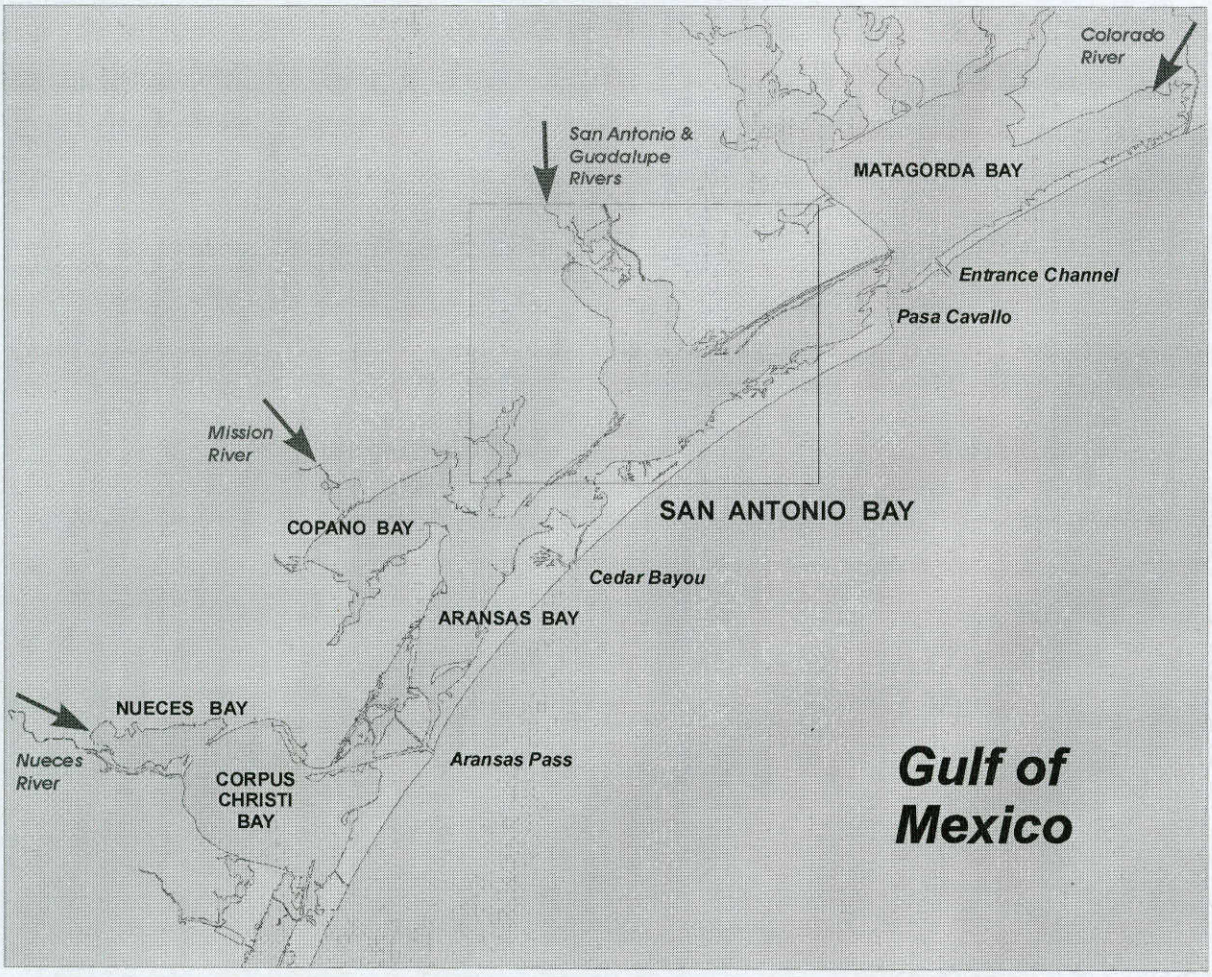

Figure 3 - A portion of the lower Texas coast showing several of the principal bays and riverine inflows.

south and Pass Cavallo/Entrance Channel on the north. (Indeed, the Laguna Madre, which lies off the map of Fig. 3 to the south, could be argued to be a part of this superestuary, since the entire system is connected.) Even if San Antonio Bay is considered as a single estuarine system, as will be done in the remainder of this missive, the larger view is important as a reminder that the bay is potentially influenced by the systems upcoast and downcoast, as well as by its own inflow and circulations. Like many of the Texas bays, San Antonio may be viewed as a physiographic merging of the sound with axis parallel to the coast, lying behind the barrier island chain, and the "drowned river valley" estuary following the drainage of the principal river, more or less perpendicular to the coast. The inland boundary of the coastal sound is the Ingleside ridge, a remnant of a Pleistocene shoreline (e.g., Blue et al., 2002).

Perhaps the most important geomorphological feature of San Antonio Bay is that it has no direct connection with the sea. The influence of the ocean, notably tides and salinity intrusion, is exerted through the tidal inlets of Pass Cavallo (and the Entrance Channel) to the north, and Aransas Pass to the south. Pass Cavallo, once one of the most energetic inlets on the coast, has shoaled considerably due to creation of the Matagorda Entrance Channel and its associated tidal capture. Aransas Pass has been stabilized for more than a century. Both of these inlets have small cross sections in comparison to the surface area of the bays to which they connect, so they behave as ports or ajutages in propagating the tide, see Section 2.2, below. Cedar Bayou, in Mesquite Bay, lies closer to San Antonio Bay than Aransas Pass or the Pass Cavallo complex, but is much smaller in cross section, therefore minor in comparison, and has been chronically closed since the 1970's, see Ward (2010a).

The bathymetry of San Antonio Bay is depicted in Figures 4 and 5. The first of these, Fig. 4, displays bathymetry in the conventional method of isopleths of depth based upon soundings distributed throughout the bay, in this case soundings of the National Ocean Service (née Coast & Geodetic Survey) from historical navigation charts. The second of these, Fig. 5, is a color-coded raster image based upon all data from five surveys from the period 1934-35, compiled by the National Ocean Service. This data compilation was undertaken by the NOAA Special Projects Office, to develop a digital elevation model (DEM) for San Antonio Bay, as a part of a project to build DEM's for each of the principal estuaries of the U.S. The datum is mean lower

low water (19-year tidal epoch). While in principle, the composited survey data underlying the raster image of Fig. 5 is much denser than the navigation chart soundings upon which Fig. 4 is based, it is not clear exactly how the various bathymetric transects were reconciled, and some of the peculiar linear features of Fig. 5 may be artifacts of this compositing (which, among other things, involves triangular linear interpolation).

Both depictions are consistent in their illustration of the main bathymetric features of San Antonio Bay. First, San Antonio Bay is shallow, its natural depths being less than 2 m, with the deepest sections in the southern half of the bay, mainly south of the Gulf Intracoastal Waterway (GIWW). Second, the lower part of San Antonio Bay is bisected by Panther Island Reef, a linear reef running almost north by west from Panther Point on Matagorda Island. Third, there is a significant bathymetric contraction in the upper bay consisting of a complex of reefs and shoals, running roughly west by south from Mosquito Point, somewhat better shown in the raster image of Fig. 5 than by the isobaths of Fig. 4. (The bathymetry of Fig. 5 is essentially that of the bay in 1934-35, though modern spoil islands along the Victoria canal and the GIWW are shown. The bathymetry of Fig. 4, based on more recent navigation charts, may include later soundings after the extensive oyster dredging of the 1950's and 1960's.) Finally, at either end of the segment south of the GIWW, connecting San Antonio Bay with the systems to the east (Espiritu Santo) and to the west (Ayres and Mesquite Bays) there are major constrictions composed of reefs and bars.

Corollary to the lack of an inlet to the sea, San Antonio Bay does not have a deep-draft ship channel, an important factor in the salination of the more industrialized estuaries on the Texas coast, especially to the north. However, there are two dredged canals in the bay, shown in Fig. 4. The GIWW crosses the bay following the dividing line between the fluvial estuary to the north and the coastal sound to the south. The San Antonio Bay reach of the GIWW has been in place since about 1940. Its original project dimensions were 9 x 100 ft (2.7 x 30.5 m), but for almost all of the postwar years, i.e., since 1949, the dimensions have been 12 x 125 ft (3.7 x 38.1 m). The Victoria Barge Canal was dredged northwest by north along the east shore in 1951-53 to project dimensions of 9 x 100 ft, then was enlarged to 12 x 125 ft in 1995-2000.

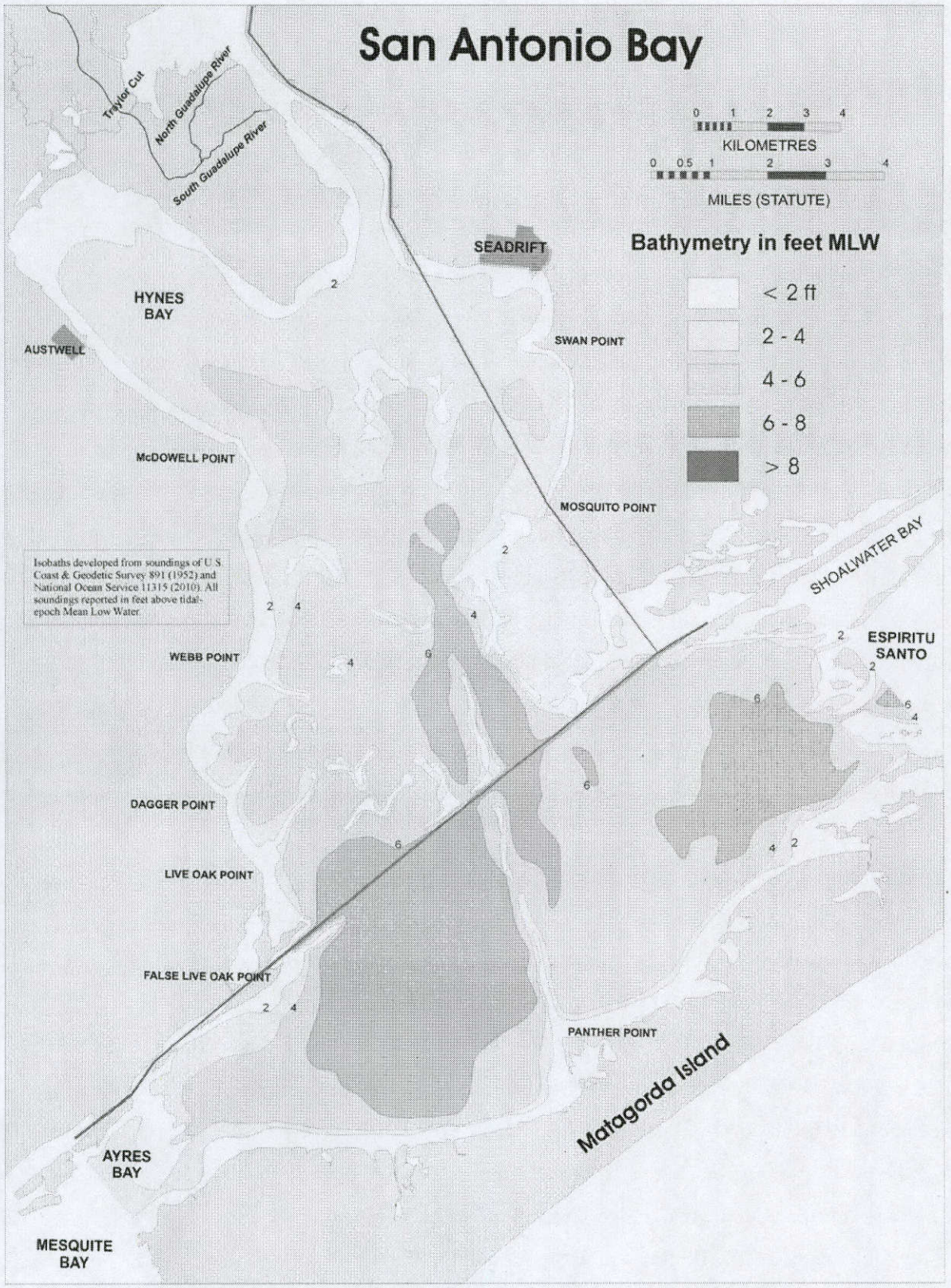

Figure 4 - Bathymetry of San Antonio Bay. Contours from National Ocean Service soundings

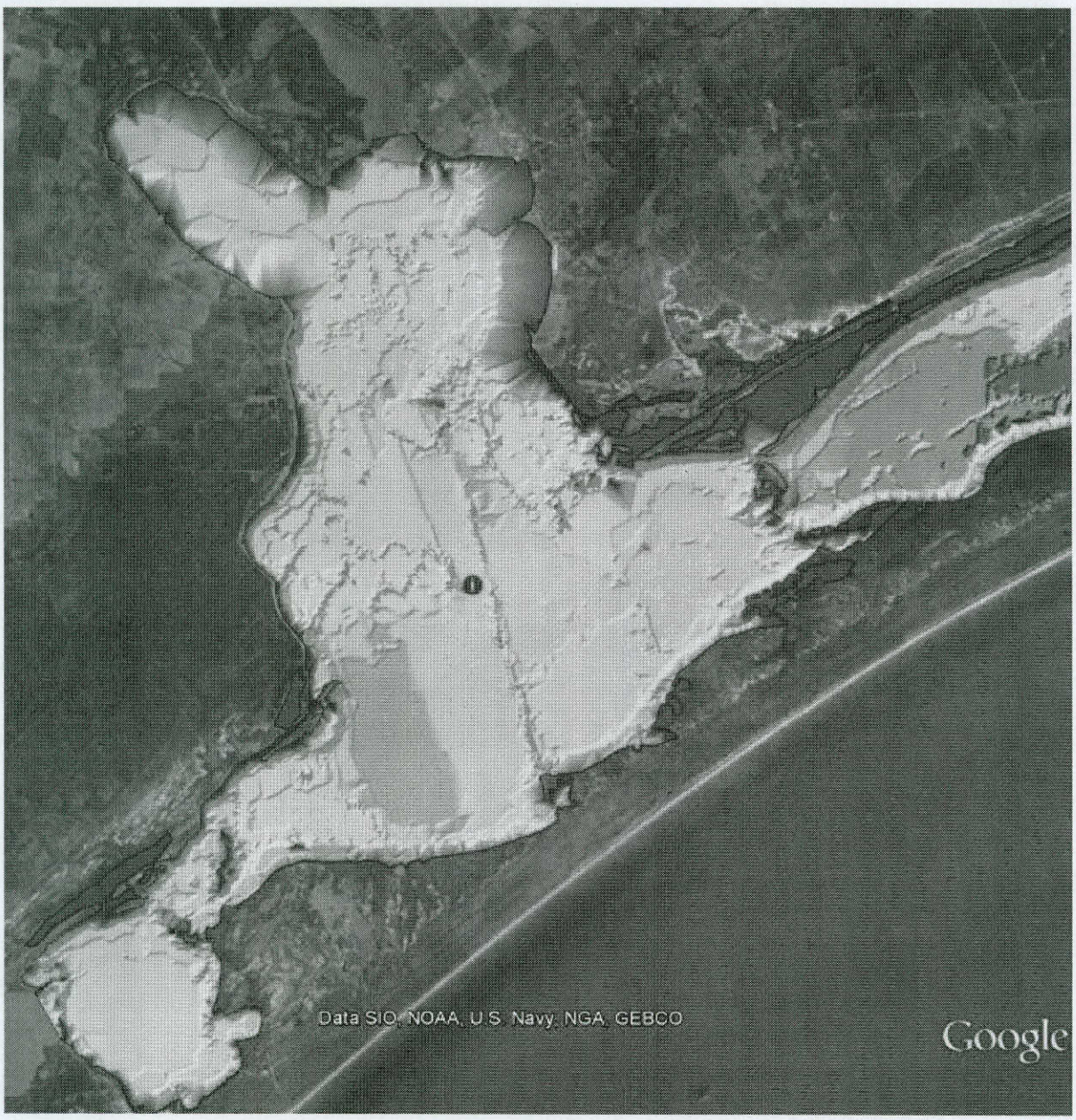

Figure 5 - Raster image of San Antonio Bay bathymetry

For the purpose of data analysis, it is useful to subdivide San Antonio Bay into segments that have some relation to physiography. One such segmentation is shown in Figure 6. Physical dimensions of these segments are given in Table 3. The basic philosophy underlying the delineation of such segments is to separate the bay into regions, each of which has some

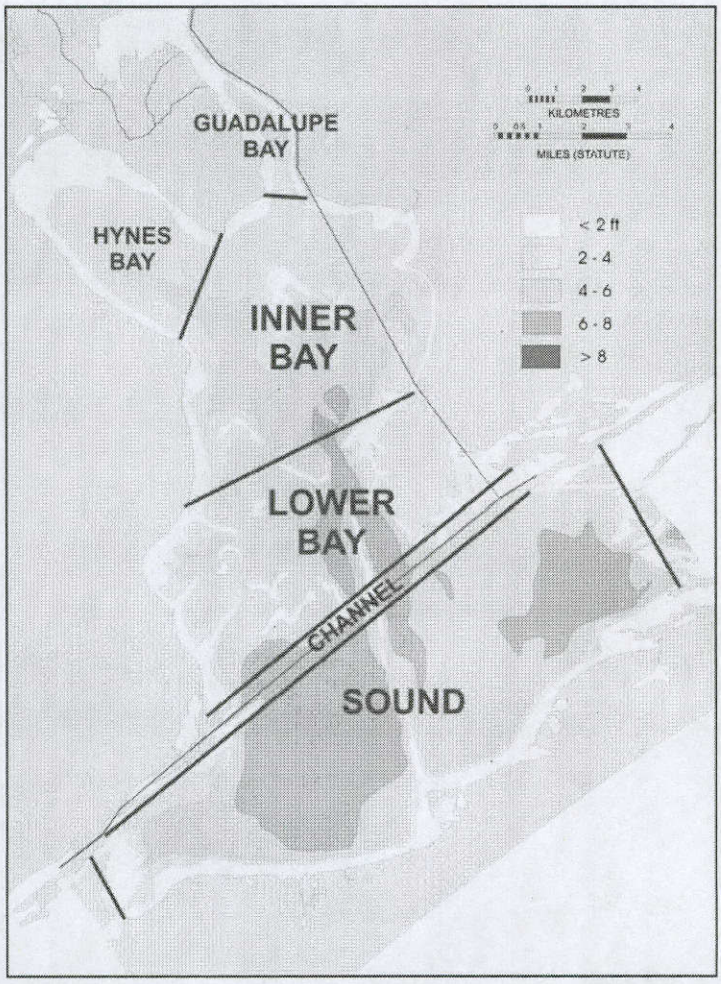

Figure 6 - Segmentation of San Antonio Bay

characteristic feature of transport or mixing that is quasi-homogeneous within that region but different from the adjacent regions. Thus the Inner Bay* segment is separated from the Lower Bay segment by the reef complex extending from Mosquito Point to Webb Point, since this reef complex would impede circulation and exchange. Similarly, Hynes Bay and Guadalupe Bay are separated by the Guadalupe delta, creating a semi-enclosed geometry that creates a

* "Upper Bay" would be a better term in contradistinction to "Lower Bay" but has already been used in other studies of San Antonio Bay to designate the entire region north of the GIWW.

Table 3
Physical dimensions of San Antonio Bay segments

	Surface area (10^6 m^2)	*Volume* (Mm^3)		*Surface area* (10^6 m^2)	*Volume* (Mm^3)
Guadalupe Bay	15.8	28.7	Channel	19.8	27.0
Hynes Bay	31.0	61.7	Sound	135.2	652.0
Inner Bay	74.2	224.8			
Lower Bay	69.2	258.7	Total bay	345.2	1252.8

physiographic identity as subbays. The Sound segment is affected by exchange with the sound upcoast and downcoast from San Antonio Bay, so this segment is treated separately from the Lower Bay Segment. The motivation and procedures for using physiography and hydrography to subdivide an estuary into segments are discussed by Ward and Armstrong (1992). This segmentation of Fig. 6 was used in the analysis of blue crab data from San Antonio Bay in Ward (2012).

2.2 Salinity intrusion processes in San Antonio Bay

As noted in Chapter 1, any process that transports seawater into the bounds of the estuary is a potential mechanism for salinity intrusion. Generally, the processes that entail movement of larger volumes of water over longer time scales are most effective in salinity intrusion, because the time of residence of the seawater in the estuary determines how much will be mixed with fresher waters by turbulence. There are two classes of process operating in San Antonio Bay potentially capable of substantial salinity intrusion: (1) tidal and quasi-tidal influxes; (2) wind-driven transports from the sea into the estuary.

Figure 7 displays measured water levels in the San Antonio Bay vicinity during one month (June 2009), selected because it was relatively free of meteorological disturbances. Figure 8 graphs the

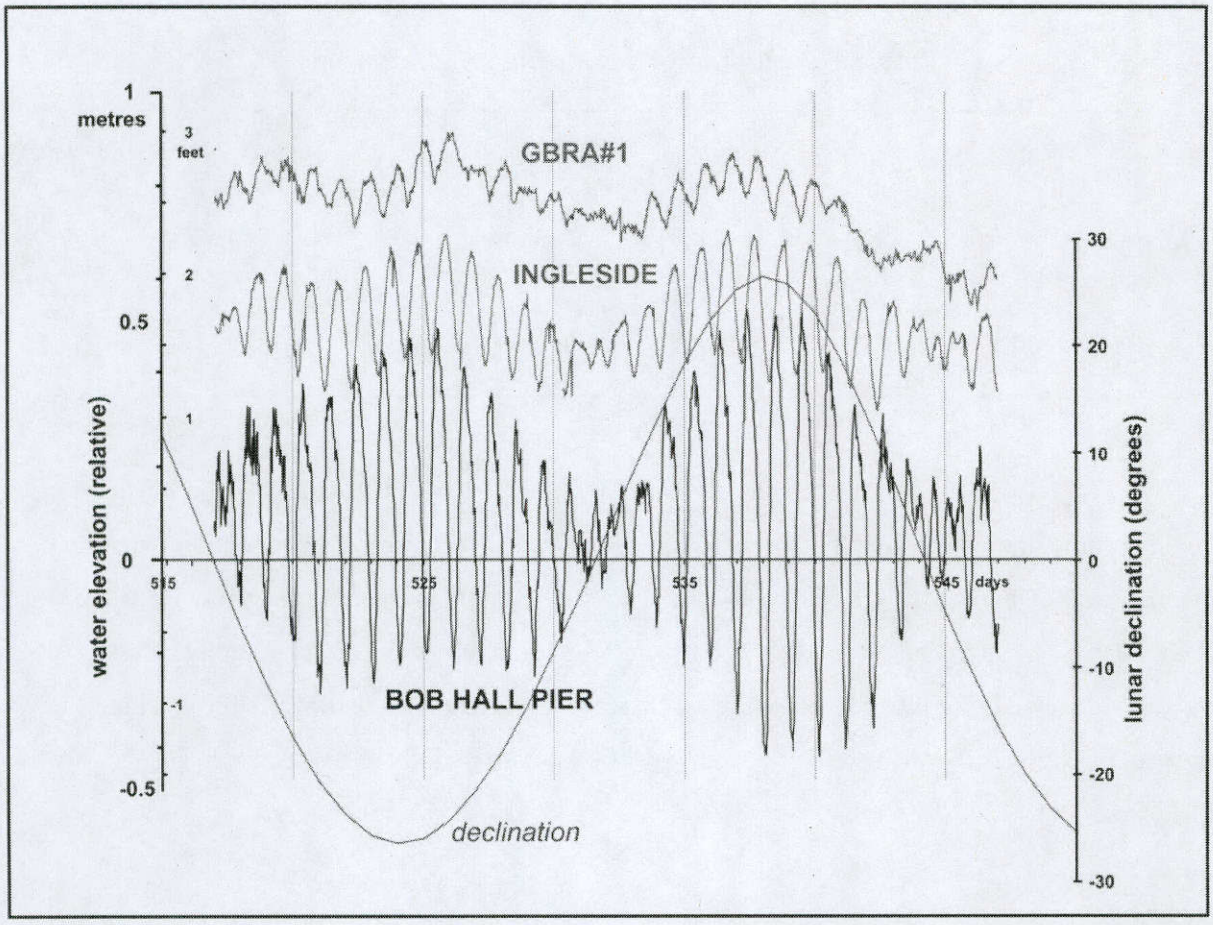

Figure 7 - Recorded tidal variation at stations in Coastal Bend bays, June 2009, see text. Curves are shifted vertically by arbitrary amounts to improve readability.

same data after being subjected to a sliding 25-hour average. Together these figures exemplify some of the propertiess of tides in San Antonio Bay. Features of the Gulf of Mexico tide, Bob Hall Pier in Fig. 7, abstracted from the survey of Ward (1997), include:

- The range of the tide in the Gulf of Mexico varies substantially over a period of about two weeks, see Bob Hall Pier in Fig. 7.
- When the range is maximal, the tide has a 24.8-hour periodicity. (This is the length of the *lunar day*.) This is informally called the "diurnal mode" of the tide.
- When the range is minimal, the tide has a 12.4-hour periodicity. This is informally called the "semi-diurnal mode" of the tide.

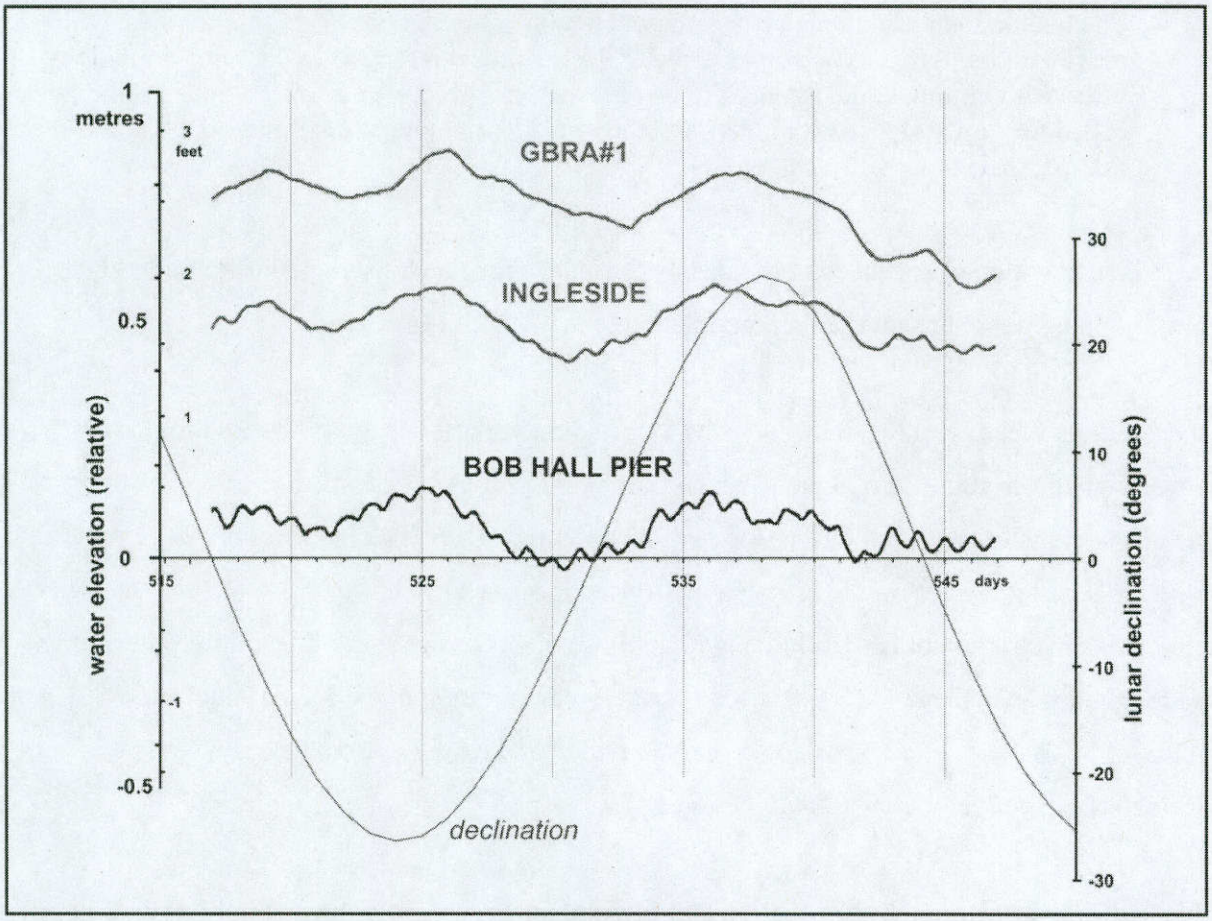

Figure 8 - Same as Fig. 7, but subjected to 25-hour sliding average.

- The average water level varies between the times of the diurnal and semi-diurnal modes with a periodicity of about two weeks. This variation in mean water level is referred to as the "fortnightly tide," shown in Fig.8.
- The range of the tide is closely correlated with the *magnitude* of declination of the moon, i.e., the angle of the moon above or below the equatorial plane of the earth. The greatest declination is the angle between the equatorial plane of the earth and the orbital plane of the moon (which varies slowly as the orbital plane rotates, with a period of about 18.6 years). During its one-month orbit, the moon's declination ranges from a maximum (positive) declination at the top of its orbit to a maximum (but negative) at the bottom of the orbit, passing through zero declination as it crosses the earth's equatorial plane. Lunar declination is plotted in Fig. 7.

- The maxima in absolute value of lunar declination correspond to the diurnal tides, with maximal tidal range. The zeroes of lunar declination correspond to the semi-diurnal tides, with minimal tidal range. For this reason, the diurnal mode of the tide is sometimes called the "great-declination tide," and the semi-diurnal mode, the "small-declination tide."

There is no mention of spring or neap tides, because, despite much local misinformation to the contrary, lunar phase has little effect on tidal range in the Gulf of Mexico.

One additional feature of the Gulf tide is its longer-term variation, exposed by a sliding average of water-level variation over 29 days, which removes most of the periodicities of Figs. 7 and 8. Such an average of each year of the Bob Hall Pier record, in turn averaged day-by-day over the 1990-2010 period, results in the mean annual variation shown in Figure 9. This is the "secular semi-annual" variation of the Gulf tide, with high waters in spring and fall, and low waters in summer and winter. There is considerable year-to-year variation in the secular tide*, as indicated by the plots of a few selected years in Fig. 9, and by the seasonal extrema in water levels for each year in the 1990-2010 period.

This Gulf tide is distorted by attenuation and filtering as it passes into the Coastal Bend estuary system. The summary of tidal mechanics in Chapter 1 is applicable in general to a generic estuary. A peculiar physiographic element of the coastal bend estuaries is the connection to the sea through extremely short and narrow inlets, such as Pass Cavallo and Aransas Pass. Such a short, narrow inlet behaves more like an ajutage between a large driving body of water (the sea) and a smaller reservoir (the bay) in co-oscillation with the larger. Unlike a large, horn-shaped estuary such as Delaware Bay or Chesapeake Bay, in which the tide is attenuated and transformed from progressive to standing wave from the mouth over a considerable distance inland, in a lagoonal estuary with a small inlet, this transformation is concentrated in the inlet itself. Inside the lagoon, the tide is uniform and synchronous, a standing wave nearly everywhere. The energy of the tide is dissipated in passage through the inlet. This attenuation is

* The secular variation is poorly understood, and may include effects of nonastronomical factors, so the term "tide" must be qualified.

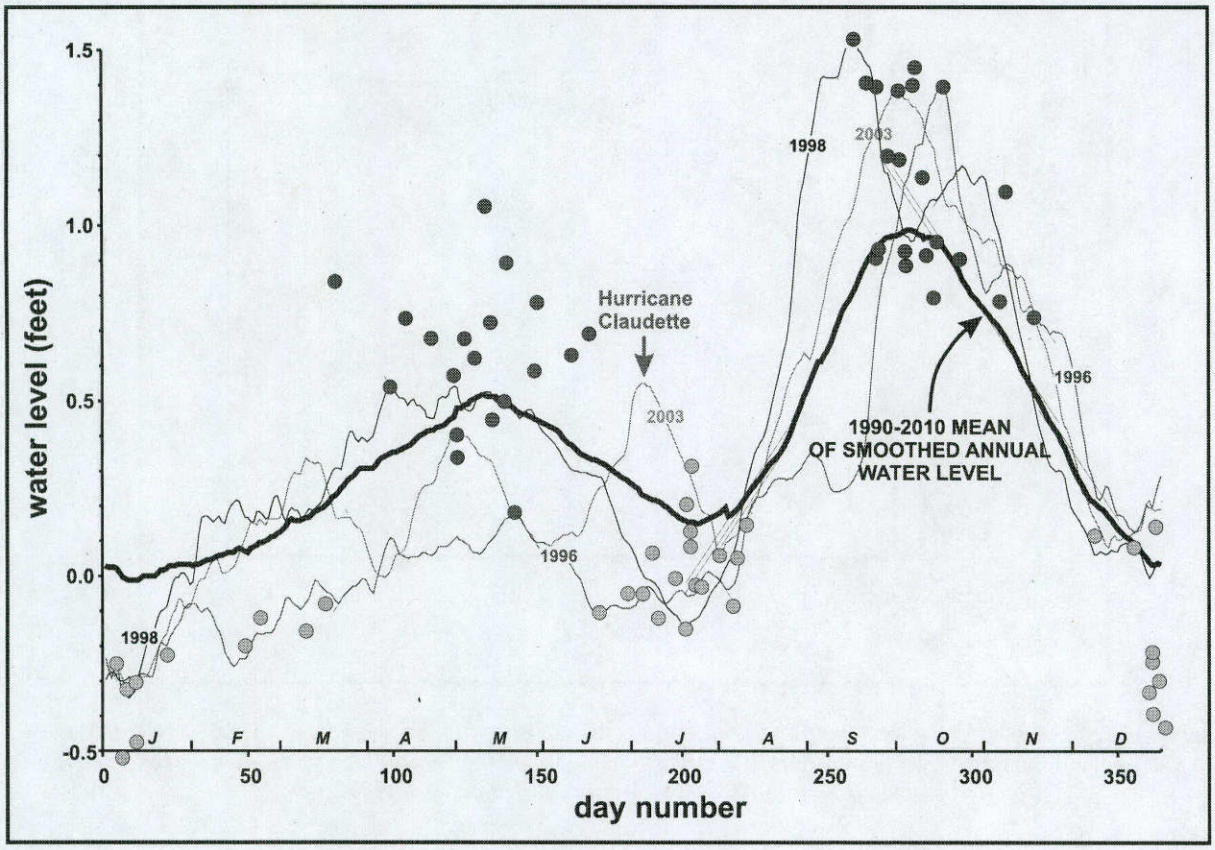

Figure 9 - Annual water-level variation at Bob Hall Pier after 29-day running mean, 1990-2010 average and selected years. Extrema of individual years plotted as red circles (maxima) and blue circles (minima).

very much frequency- (i.e., period-) dependent. A theoretical hydraulic model for a short inlet connected a bay to the sea is presented in Ward (1997), and a specific solution for a bay of dimensions of the Corpus Christi/Aransas-Copano system with an inlet of dimensions of Aransas Pass is shown in Figure 10. The diurnal tide is seen to be reduced in amplitude about 74%. This is approximately the reduction in range of the tide at Ingleside to that at Bob Hall Pier in Fig. 7.

The semidiurnal tide is reduced even more, about 86%, upon passage through the inlet. In Fig. 7, the semi-diurnal tide is barely discernible as a ripple in the Bob Hall tide, most apparent at small declination, and at Ingleside it is virtually absent. The fortnightly tide, in contrast, passes

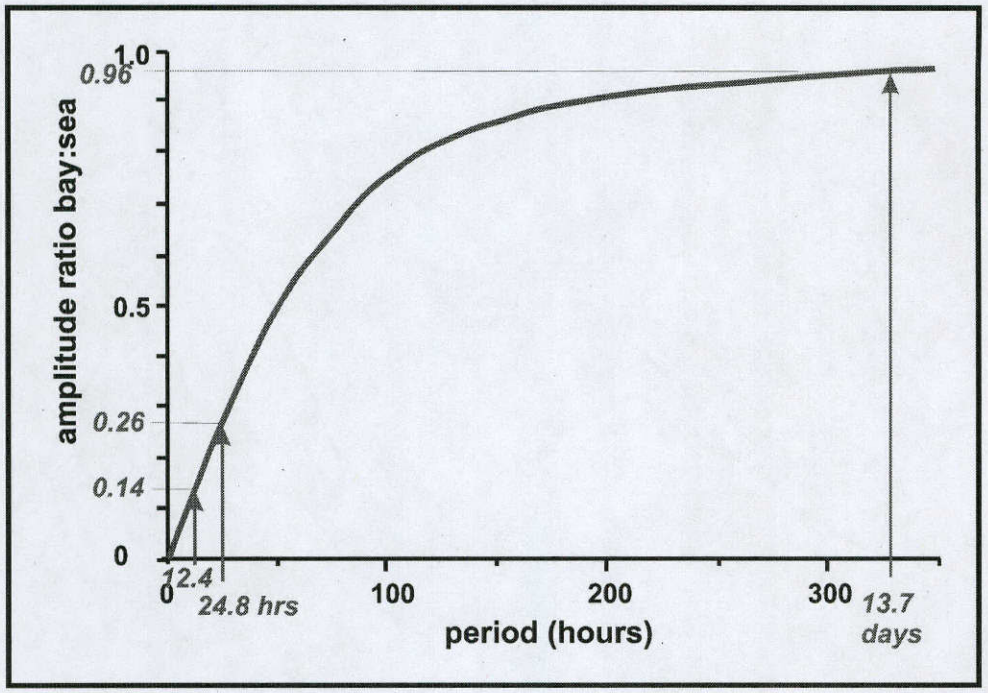

Figure 10 - Theoretical relation of ratio of tidal amplitude inside bay to forcing tide in the sea as a function of tidal period, for inlet with dimensions of Aransas Pass, connecting co-oscillating bay of surface area of Coastal Bend bays to sea. Re-drawn from Ward (1997).

through the inlet with only 4% attenuation according to Fig. 10. This component is exposed by the 25-hr sliding average of Fig. 8, where it is seen that the resulting water-level trace is practically identical at Bob Hall Pier and Ingleside.* The effect of inlets in filtering the higher frequencies in the tide is analogous to the effect of a small port in a stilling well.

Within the coastal bend estuarine system, there are additional small inlets connecting the component bays, for example, Nueces Pass between Corpus Christi Bay and Nueces Bay, and Copano Pass between Aransas Bay and Copano Bay. Each of these acts similarly as an ajutage between two large reservoirs, so that the higher frequencies of the tide are attenuated even more as it propagates from one to the other. Thus the Aransas Bay tide is attenuated with its passage

* There is a small diurnal ripple in these tides due to some of the diurnal species being incommensurate with the 25-hr period of the averaging. Consistent with Fig. 10, this is greatly attenuated from Bob Hall Pier to Ingleside.

through Carlos Bay into San Antonio Bay. This is evidenced by the water-level at GBRA#1, in Lower San Antonio Bay just off from Live Oak Point, shown in Fig. 7. Again, the diurnal component is significantly attenuated, and what is left of the semi-diurnal nearly eliminated.

The diurnal tidal range in San Antonio Bay is about 0.1 - 0.4 ft depending on lunar declination (Fig. 7). This corresponds to a range of tidal prism of 10 – 42 Mm^3, *at most* about 3% of the volume of the bay. The fortnightly tide has a range on the order of 0.5 ft, with an associated prism on the order of 50 Mm^3. Unlike the diurnal tide, whose prism enters the bay daily, the fortnightly prism enters the bay over a seven-day period. This affords a greater potential for the prism to be mixed with estuarine water, thereby raising the overall salinity in the estuary. The range of the secular semi-annual tide is much greater, with a prism of about 1500 Mm^3, varying perhaps a factor of two above or below depending upon the year. Thus over a four-month period, this component of the tide is capable of equalling the volume of San Antonio Bay (cf. Table 3) and in the process being mixed throughout the system. If the bay is initially fresh, but receives no additional freshwater inflow, this exchange alone would raise the salinity of the bay to 3/4 seawater after one year. If the bay were initially at half seawater, after one year this exchange would raise its salinity to 7/8 seawater.

The second class of processes that transport seawater into San Antonio Bay is water movement driven by the wind. Wind affects the movement and mixing of coastal waters in a number of ways, both direct and indirect. The wind stress on the water surface effects a direct movement of surface waters in the direction of the wind. These currents can be modified by other factors, such as bathymetry and the rotation of the earth. Wind stress also generates waves, whose breaking is an important source of turbulence and mixing. The net movement of water under the influence of wind leads to accumulations or depletions of water volume in different areas, in turn producing variations in the height of the water surface, which drives currents from high water to low water. These currents, whose direction and magnitude may have no obvious relation to wind velocity, are an example of indirect transport due to wind.

The most dramatic routine wind-driven water movement is in response to the changing winds associated with a frontal passage. It will be recalled that a front is a boundary between dissimilar

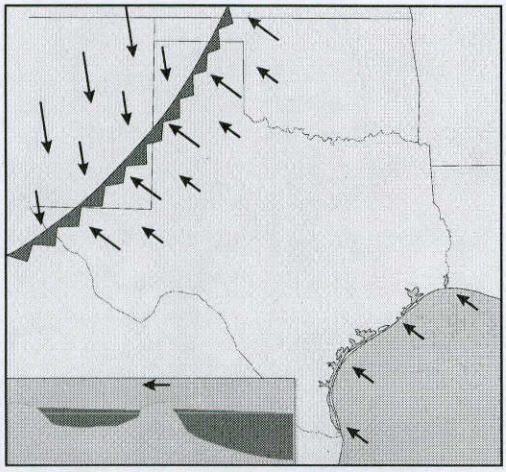

(a) Normal onshore (S or SE) winds along coast. Front enters state.

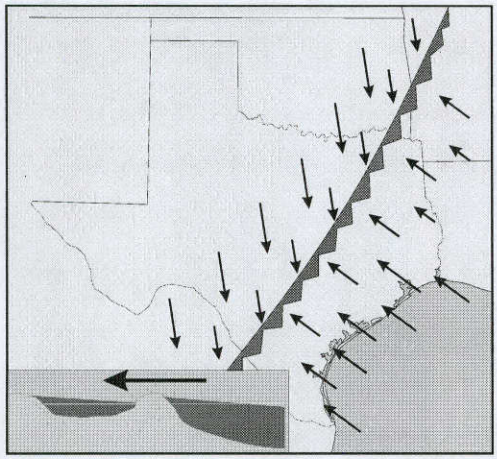

(b) Front approaches coast, enhancing onshore flow.

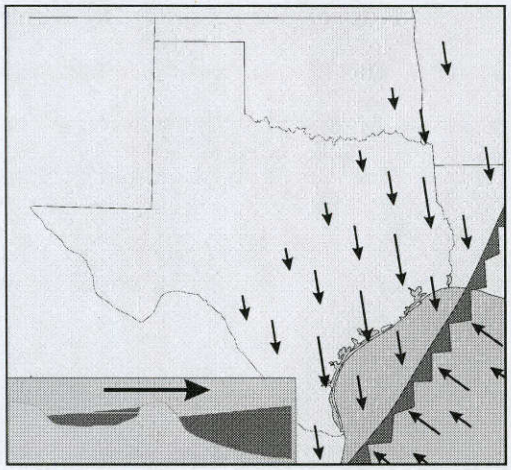

(c) Front passes into NW Gulf of Mexico, entire state under N winds.

Figure 11 - Schematic of effect of frontal passage on coastal water levels and associated flows through inlets

airmasses, typically differing in temperature or humidity (or both). Fronts traverse the state generally from the NW quadrant to the SE, and are part of the circulation of a much larger synoptic system, typically anchored in a cyclone in the northern tier of states. The intensity of the cyclone, its rate of movement, and other structural features dictate the properties of the surface front in Texas, including direction and rate of movement.

Figure 11 is a highly idealized schematic of the effect of a frontal passage on water levels and water transport in the Texas coastal zone. The water-surface variation across the barrier island is depicted in cross section in the small inset panels of this figure. Generally, the frontal zone is a region of low-level convergence, see Fig. 11(a). As the front approaches the coast, the normal onshore windflow, i.e., from the SE quadrant, is enhanced, resulting in a set-up of water level along the coast and on the inland side of the bays, Fig. 11(b). This set-up creates a water-level difference across the barrier island, with higher water on the seaward side, thus driving a flow through the inlets from the Gulf into the bays, see the inset panel of Fig. 11(b). It is the time period during the approach of the front in which seawater is forced into the bays by the enhanced onshore flow that is responsible for salinity intrusion. Once the front passes the coast, winds turn sharply to north* setting down water levels where they were set-up before the frontal passage, viz. along the inland margins of the bays and along the Gulf beach, Fig. 11(c). This creates a difference in water-elevation across the barrier island, but in the opposite direction of Fig. 11(b), driving a flow through the inlets from the bay into the sea. This phase of the frontal passage response is salinity extrusion, and is addressed in Section 2.3, below.

About 50 frontal passages occur per year in Texas of varying speeds, pressure gradients and associated weather. The volume of sea water forced into the bay with the approach of the front can be more than half the volume of the bay, particularly on the upper Texas coast where fronts are typically more energetic and the inlets of the bays are larger. On the lower coast, while the volume of seawater intrusion is typically somewhat smaller, a frontal passage will nonetheless obliterate the astronomical tide, and remains an important agency for Gulf water exchange and

*The reader is reminded that the convention for wind direction is that *from which* the wind flows, in contradistinction to the convention for water current direction *to which* the current flows.

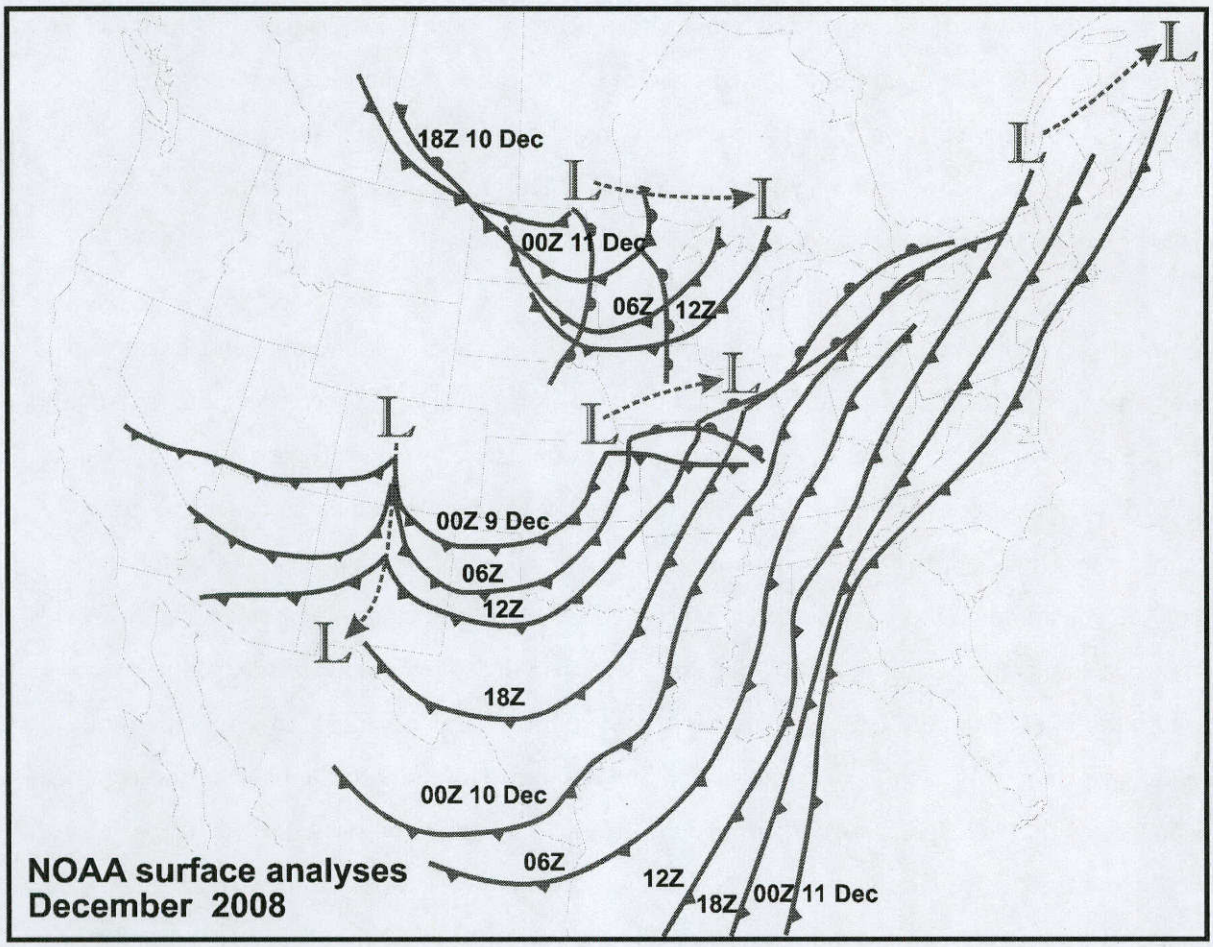

Figure 12 - Surface front positions at 6-hour intervals, 9-11 December

salinity intrusion. Detail on the hydrography of frontal passages in the Coastal Bend area is presented by Ward (1997).

As an illustrative example of the response of San Antonio Bay to a frontal passage, an event in early December 2008 is examined. The time series of surface fronts, abstracted from the surface analyses of the National Weather Service, is shown in Figure 12. The frontal passage of 10 December was driven by a developing cyclone on the Great Plains that tracked eastward across the Upper Mississippi Valley. Wind velocity measured at Port O'Connor and Seadrift are shown in the upper panel of Figure 13, and the water-levels observed at two stations in the San Antonio Bay vicinity area in the lower panel of the same figure. Despite the tardy response of water level

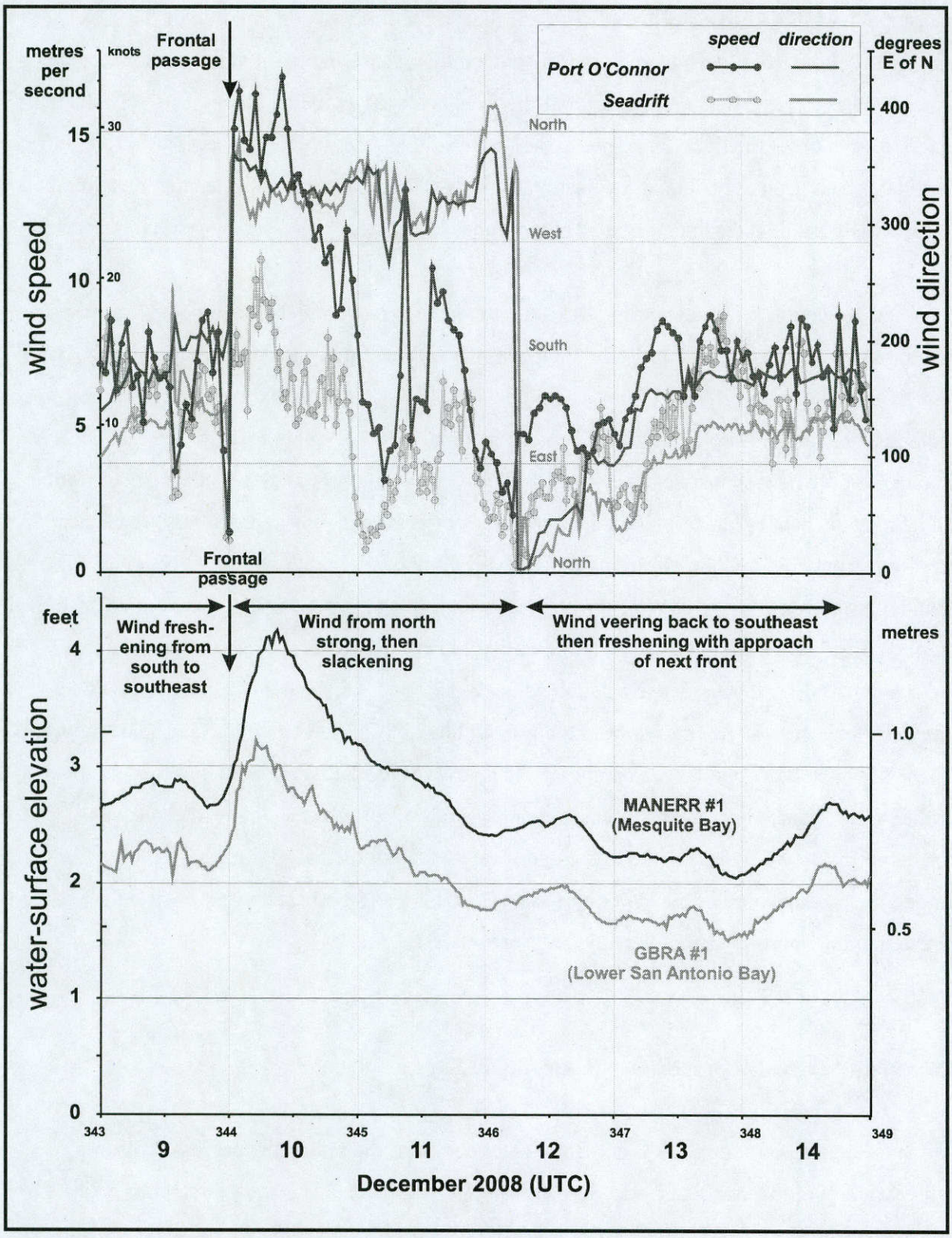

Figure 13 - Response of water level in San Antonio Bay (below) to changes in wind associated with frontal passage (above), 9-14 December 2008. Water-level plots shifted vertically to improve readability.

measured at GBRA#1 then at MANERR#1, farther south, due to a combination of the slow movement of the front from the more northward anemometers, and to inertial lag, the increase in water level associated with the approach of the front is clearly evident and ranges 1 – 1.5 ft. This is four to five times the tidal range, hence the water volume entering the bay is four to five times the tidal prism. Consideration of the examples given by Ward (1997) indicates that this volume transport is typical, and can range two or three times larger with energetic, fast-moving fronts.

As noted in Section 2.1, San Antonio Bay does not have a deepdraft ship channel. However, there are two channels whose project depths are two to three times the natural depths of the bay, namely the GIWW and the Victoria Barge Canal (see Fig. 4). Given that the density current scales as the cube of water depth (Ward and Montague, 1996), it might be expected that these channels would be responsible for enhanced salinity intrusion through this mechanism. In order for a dredged channel (or, for that matter, any locus of greater depths in an estuary) to carry a density current, the gradient in salinity must have a component parallel to the direction of the channel. In the case of the GIWW, the channel crosses the bay more-or-less perpendicular to the gradient of salinity. There is, therefore, minimal gradient in density directed along the axis of the channel to drive a density current, and where it does operate, the density current would be directed along the GIWW transverse to the longitudinal axis of San Antonio Bay. The Victoria Channel, on the other hand, does parallel the main axis of the estuary, and therefore a component of the salinity gradient would be directed along the axis of this channel. Any such density-current intrusion would be limited to the open-water reach of the barge canal, however, mainly around the eastern shore of the lower bay, because the trajectory of freshwater entering the bay is directed to the opposite side of the bay (see Section 2.3).

2.3 Salinity extrusion processes in San Antonio Bay

Any mechanism that transports water from the estuary into the sea, in the process replacing saltier water with fresher water, accomplishes salinity extrusion. There are three classes of processes that effect salinity intrusion in San Antonio Bay, (1) tides; (2) wind-driven exchanges;

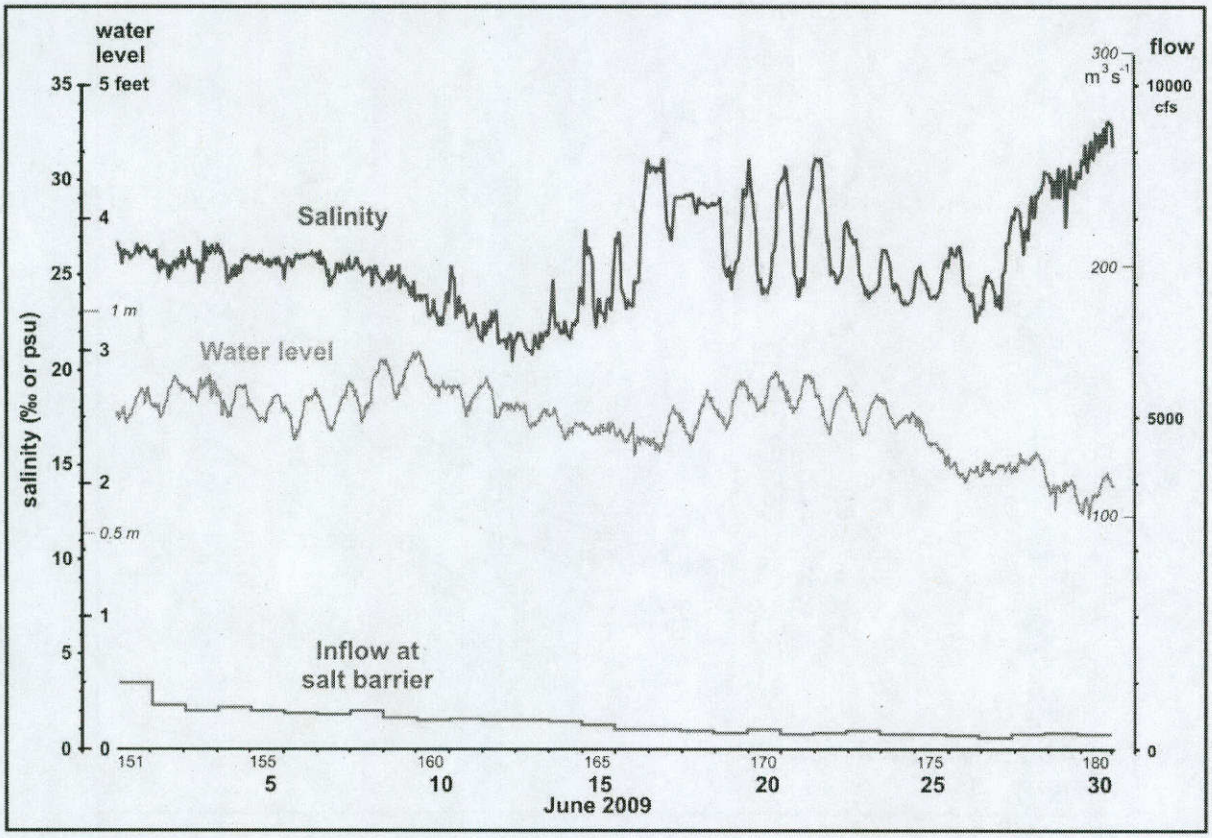

Figure 14 - Time variations of salinity and water level in San Antonio Bay, June 2009 (cf. Fig. 7) with daily inflows into estuary at salt barrier

(3) freshwater inflow. Analogous to salinity intrusion processes, it is those that entail movement of larger volumes of water over longer time scales that are most effective in salinity extrusion.

The essential fact about tidal water exchange is that it is oscillatory. On the rising tide, the tidal prism enters the bay, and on the falling tide the same volume leaves the bay. If the tidal prism were not to mix with either the water of the nearshore coastal zone or the water within the estuary, then this exchange would have no net effect on salinity within the estuary. At a point within the estuary, there would be an oscillation of salinity with transport in and out, but no net change in value from one tidal cycle to the next. It is the energy of turbulence and the associated intensity of mixing that accomplishes a net alteration in salinity. As discussed in Section 2.2, the intermixing of water in the estuary with the incoming tidal prism raises its average salinity. In

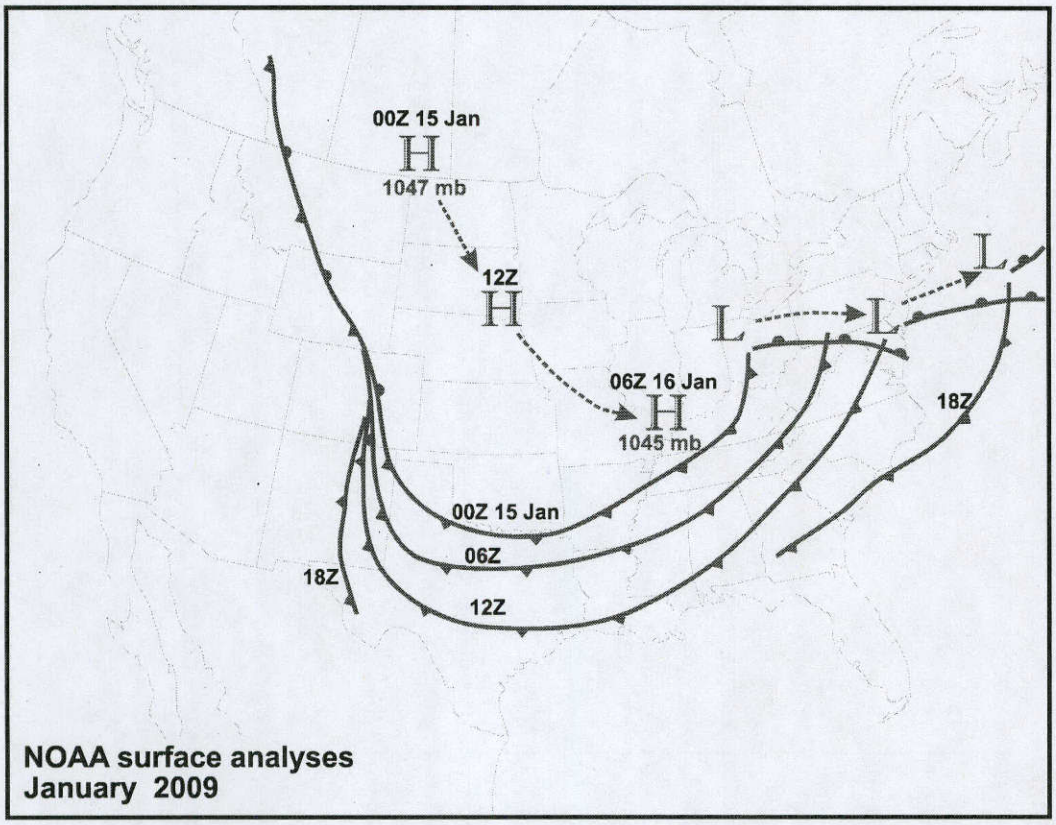

Figure 15(a) - Surface front positions 15-16 January 2009

the present context, when this same, mixed volume is now forced back into the near-coastal water, the removal of this saltier water mass reduces the average salinity of the water remaining in the estuary, and therefore represents salinity extrusion. Of course, as noted earlier, the tide is greatly attenuated with propagation into San Antonio Bay and the extent to which it departs from the harmonic variation is an indicator of the increasing variability contributed by other sources of water movement, and the extent to which turbulence is generated. To detail the mechanics of tidal prism mixing in either the estuary or the coastal zone would detour the focus of this report. These matters are surveyed by Ward and Montague (1996) with citations to the literature.

For present purposes, the salinity time signal as recorded at a robot monitor in Lower San Antonio Bay is shown in Figure 14 for the same June 2009 period selected in Fig. 7 as an exemplar of astronomical tide in San Antonio Bay with minimal nonastronomical perturbations.

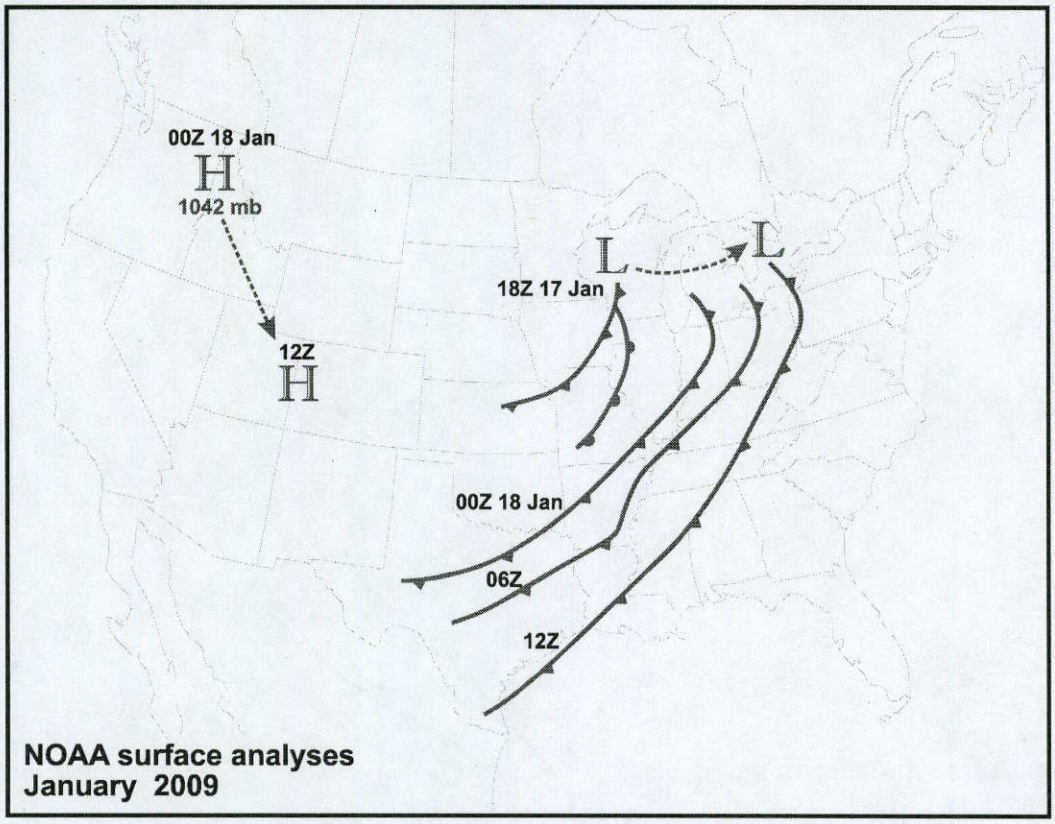

Figure 15(b) - Surface front positions 17-18 January 2009

Despite the relatively clean tidal oscillation of water level, there is only a brief period, 20-25 June, when salinity exhibits a clear, undistorted tidal variation.

As was the case with intrusion, the effects of winds are much greater than those of the tide in salinity extrusion in San Antonio Bay. This is in part due to the greater volumes of water exchanged, compared to tides, but also due to the longer time scales. There is a definite asymmetry in the extrusion versus intrusion processes in this regard. Extrusion, particularly as effected by frontal passages, tends to be compressed in time, with greater rates of flow from the bay into the sea. Intrusion, in contrast, generally requires longer, and therefore may be the result of multiple atmospheric disturbances. An example is shown in Fig. 13, in which the intrusion event associated with the approach of the front occurs over about 12 hours. The extrusion event,

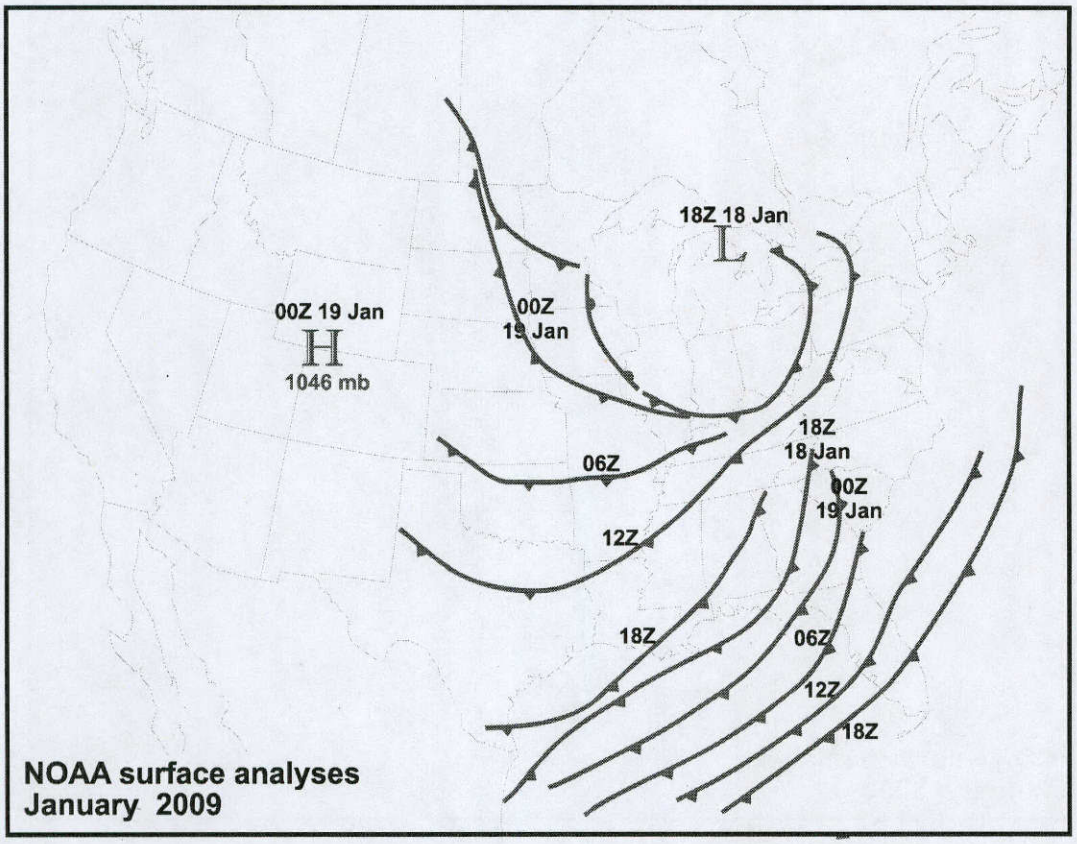

Figure 15(c) - Surface front positions 18-19 January 2009

marked by the decline in water level after the frontal passage, continues for 2-3 days. A more dramatic example is shown in Figure 15-16, in which sustained high pressure and north winds followed an initial frontal passage on 16 January, Fig. 15(a), reinforced on 18 and 19 Jan by additional surges of high pressure, Figs 15(b) and 15(c). The response of the bay to these events is shown in Fig. 16, following the same format as Fig. 13. The intrusion event was relatively modest, but the extrusion was sustained for over four days, and water levels were driven down to about three times the increase in water levels during the approach of the initial front. It should be noted that during this entire event, winds were directed from the southern quadrant only on 17 January, and were too light to effect much of an influx. Otherwise the winds were NE or NW.

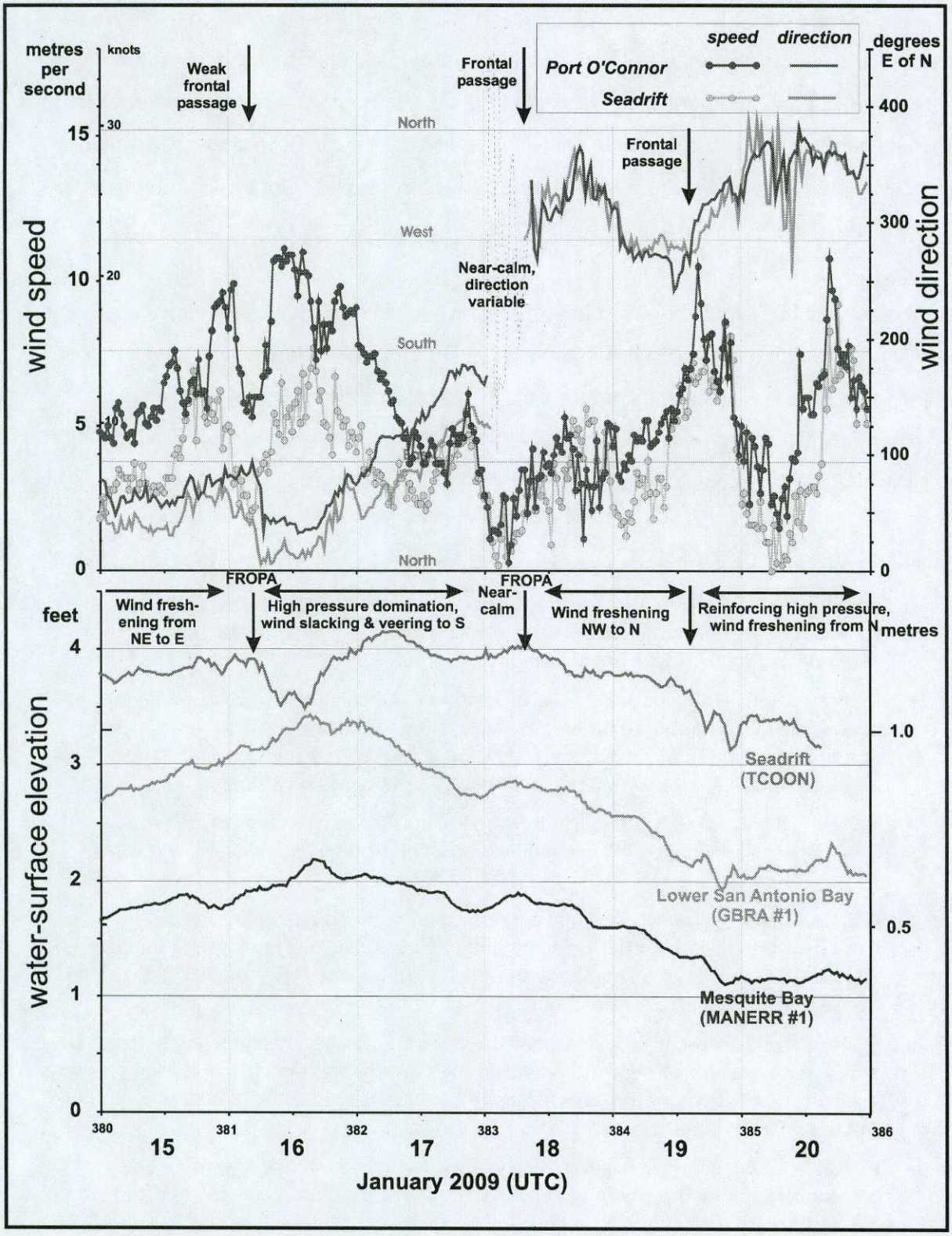

Figure 16 - Response of water level in San Antonio Bay (below) to north winds and high pressure associated with multiple frontal passages (above), 15-20 January 2009. Water-level plots shifted to improve readability.

The rise in water level during NE winds prior to 16 January might be embraced by a hopeful reader as a demonstration of the effect of Ekman transport accumulating water in the nearshore zone. This is, however, more likely the result of direct windstress from Matagorda Bay into the sound (Espiritu Santos) and thus into San Antonio Bay, see Fig. 3. Such a transport would represent seawater intrusion because it is compensated by inflows from the Gulf through the Pass Cavallo complex (including the Matagorda Entrance Channel).

As summarized in Chapter 1, freshwater inflow is the most important governing parameter for the salinity distribution in an estuary. Almost all other processes influencing the variation of salinity depend upon spatial gradients created by freshwater inflow. (Exceptions include evaporation and precipitation.) The general hydroclimatology of Texas, and of San Antonio Bay in particular, may be summarized as follows (see Ward, 2004, 2011):

- Streamflow is predominantly fed by runoff from precipitation on the land surface.
- Precipitation is almost entirely rainfall, and is produced almost entirely from deep convection, i.e. thunderstorms. The synoptic structures that stimulate thunderstorms vary with season and with position in the state.
- Rainfall declines precipitously from east to west. Depending upon the averaging period, the mean rainfall in far east Texas is about 70 inches (180 cm), and in the desert west about 10 inches (25 cm). The annual isohyets align generally with longitude meridians, except in the vicinity of the Balcones escarpment.
- Runoff is small as a fraction of rainfall, and the ratio declines from east to west. Runoff:rainfall is about 30% in the humid east and declines to about 1% in the arid west.
- Runoff volume, hence streamflow, declines even more precipitously from east to west, by more than two orders of magnitude. This means that streamflow into the estuaries declines from Sabine Lake to Laguna Madre about two orders of magnitude, from about 17,000 Mm^3yr^{-1} to about 300 Mm^3yr^{-1}.
- Because of its deep-convective origin, streamflow is flashy. A typical hydrograph of a river is a sequence of high-inflow pulses, or storm hydrographs, superposed on a low base flow. The storm hydrographs tend to cluster seasonally in both magnitude and distribution in time.
- Because of long-term variation in the synoptic triggers for thunderstorm development, there is a spatially coherent, long-term vacillation in rainfall, from wet (pluvial) to dry (drought).

Hydrological attributes of San Antonio Bay in particular include:

- The seasons of highest streamflow are spring and fall, with lowest flows in the summer.
- Almost the entirety of the freshwater input to the system enters at the head of the estuary, about 95% at the salt barrier in the Guadalupe channel, in contrast to multiple entry points characteristic of most of the Texas bays.
- San Antonio Bay is located on a climatological gradient between the humid northern coast, and the arid southern coast. On a time scale of multiple years, the bay is exposed alternately to humid and arid hydroclimatology governed by the large-scale movement of atmospheric circulation patterns.
- Lacking a direct inlet to the sea, exchange between San Antonio Bay and the Gulf of Mexico takes place through inlets relatively distant from the bay. This means that the effects of high inflows and low inflows tend to be sustained for much longer periods than is the case for bays with freer exchange.
- Inflows to the bay exhibit surges separated by periods of low flow. Over the 1942-2009 record, the magnitude of these surges has increased by about a factor of two. Droughts separating the surges of inflow have tended to increase in intensity over time. The three most intense droughts on record have occurred in the last two decades. Most intense was the drought of 2008-09.*

An overview and summary of freshwater inflow into San Antonio Bay is presented in Ward (2010b). Ten droughts exceeding one-year duration were identified in the 1942-2009 record, representing 40.5 of the 68-year period, i.e., the bay inflows are in drought conditions about 60% of the time.* The most severe drought on record is the Drought of the Fifties. (This is in contrast to the intensity of a drought, noted above.) The play in the popular press notwithstanding, this study found little association of wet versus dry conditions, as measured by departures from normal of bay inflows, with El Niño versus La Níña in the Equatorial Pacific.

Upon examination of the response of salinity indicated by data following inflow events, it becomes immediately apparent that San Antonio Bay acts as an integrator of hydrologic variability. That is, it is not the individual storm hydrograph "spikes" that engender a salinity response, but rather their cumulation over some longer duration of time. The bay's salinity

* The analysis has not been extended through 2013. Intense drought conditions were experienced in 2010-2012.

structure responds to the seasonal clustering of such hydrographs as though their cumulative volume of inflow were received as a distinct volume of inflow sustained over many weeks. These volumes of inflow have long been referred to as seasonal freshets. For analysis purposes, these are often cumulated over multiple months (e.g., Ward and Armstrong, 1992). A convenient integration time-step for suppressing the details of the hydrograph spikes and exposing the longer-term variation in flow is one month. A comparison of daily flows and the 30-day running mean is shown in Figure 17, displaying these inflow time signals for 1977-2009. These averages are antecedent means, by which is meant that the 30th value in the average is the day to which the mean value is assigned. For example, the 30-day mean value for 15 December 1977 is the average of daily values starting with 16 November and extending through 15 December. Use of the antecedent mean (rather than, say, a centered mean) is in anticipation of its use in explaining the salinity response, which of course depends only upon preceding values of flow, and none following the date of salinity measurement. It should also be observed that the signal of 30-day antecedent mean flows is made up of continuous daily values. Use of this running average time signal does not follow the traditional use of monthly flow data in hydroclimatology and in water-supply engineering. Only if the 30-day running mean is sampled on the last day of each month does it correspond to the discrete monthly record employed in these kinds of studies.* The time axes are subdivided into equal twelfths to approximate the months of the year.

* The use of one-month flows has an unfortunate property in that the time step is nonuniform due to the varying number of days in a month. This is generally a small error compared to other sources of error in hydrology.

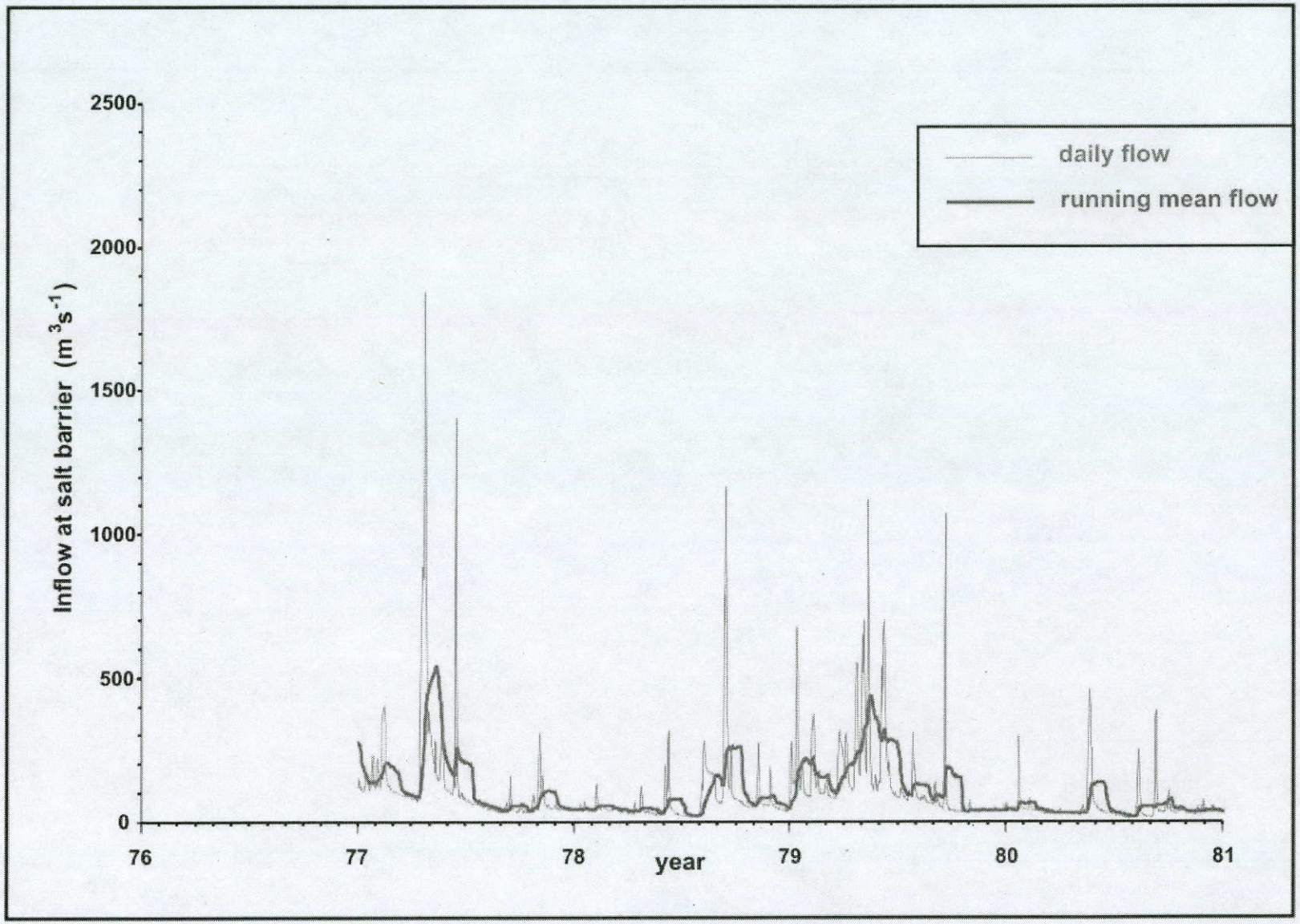

Figure 17(a) - Time series of inflow of Guadalupe at salt barrier, daily data and 30-day running mean, 1976-80

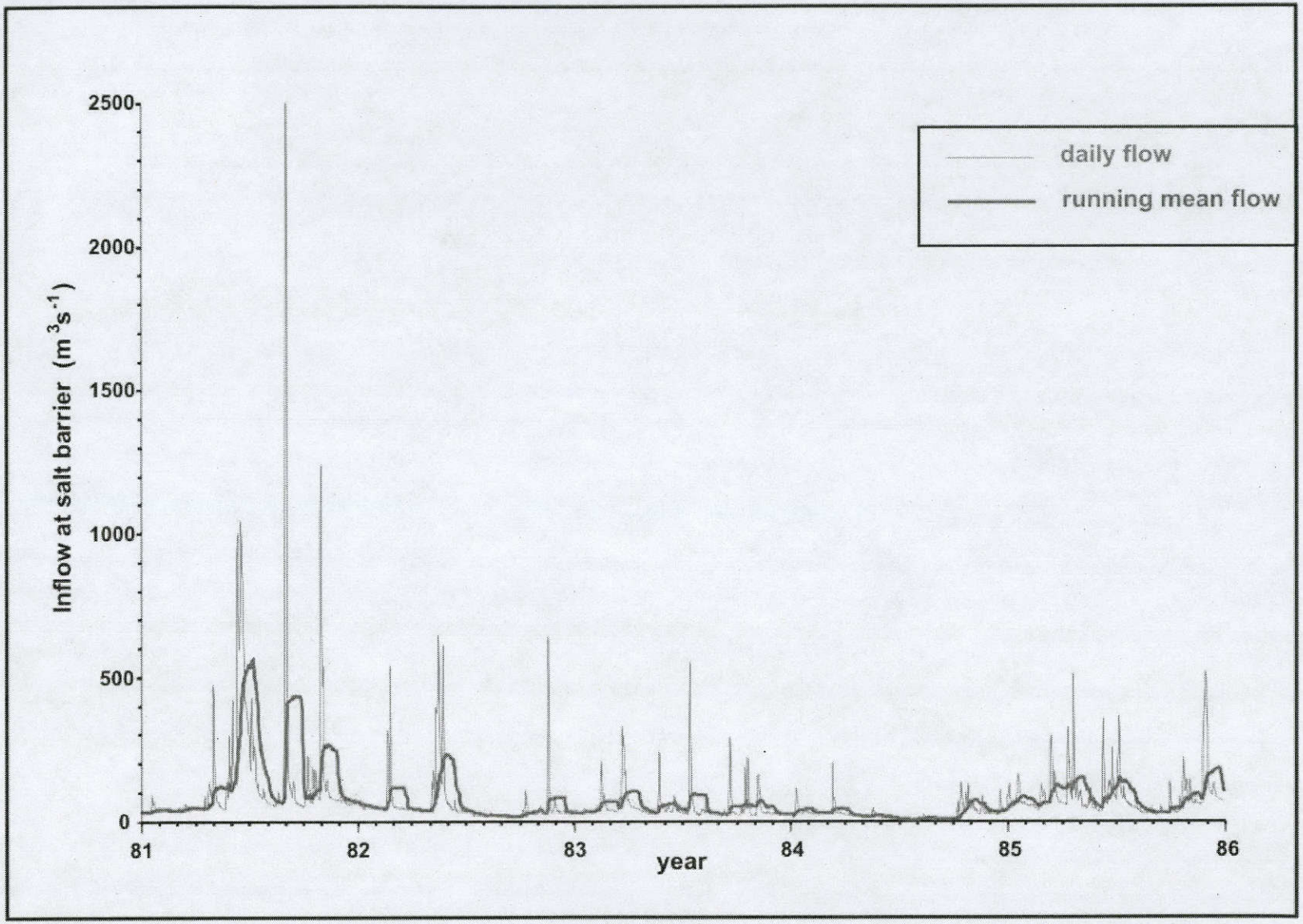

Figure 17(b) - Continued, 1981-85

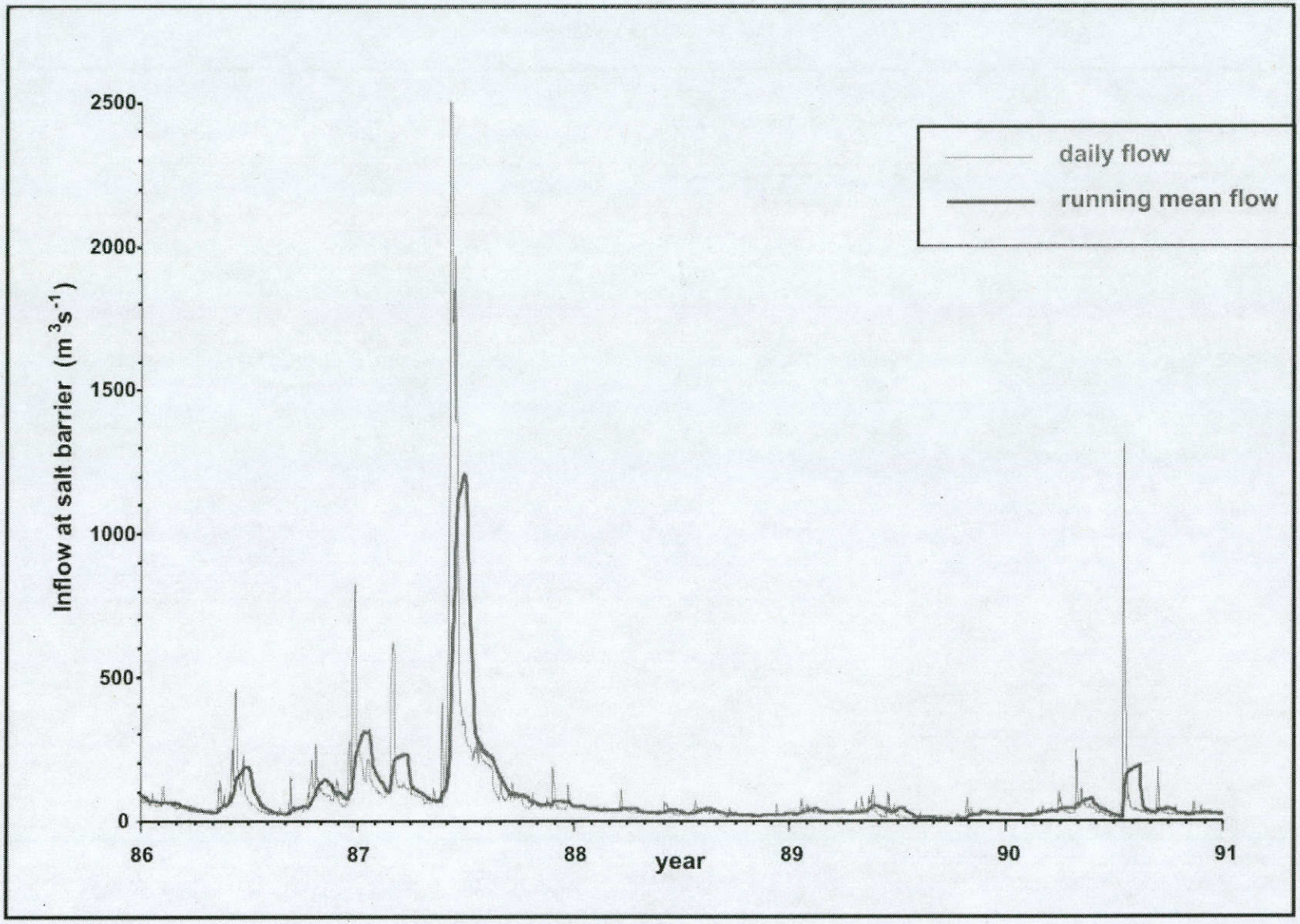

Figure 17(c) - Continued, 1986-90

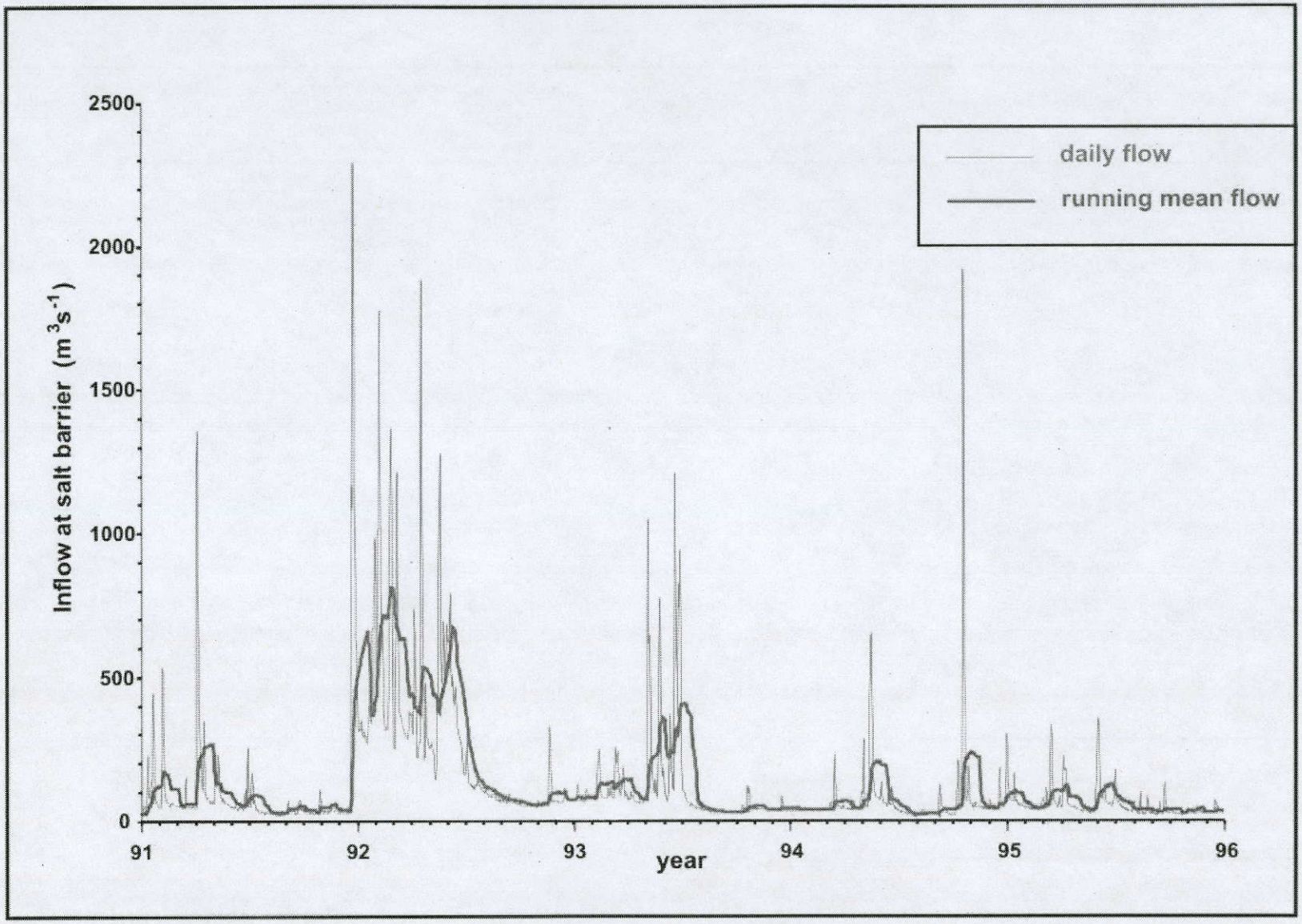

Figure 17(d) - Continued, 1991-95

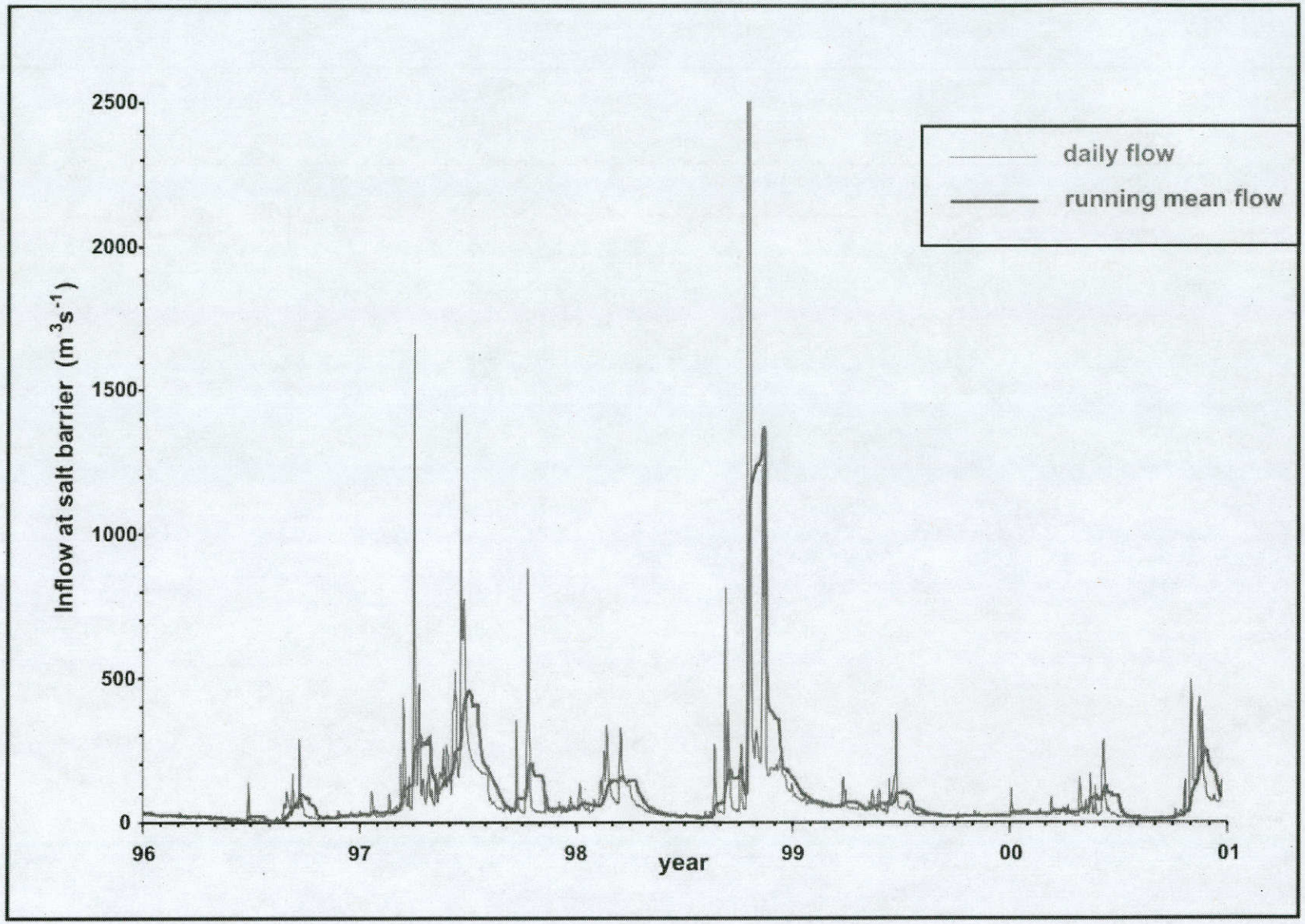

Figure 17(e) - Continued, 1996-2000

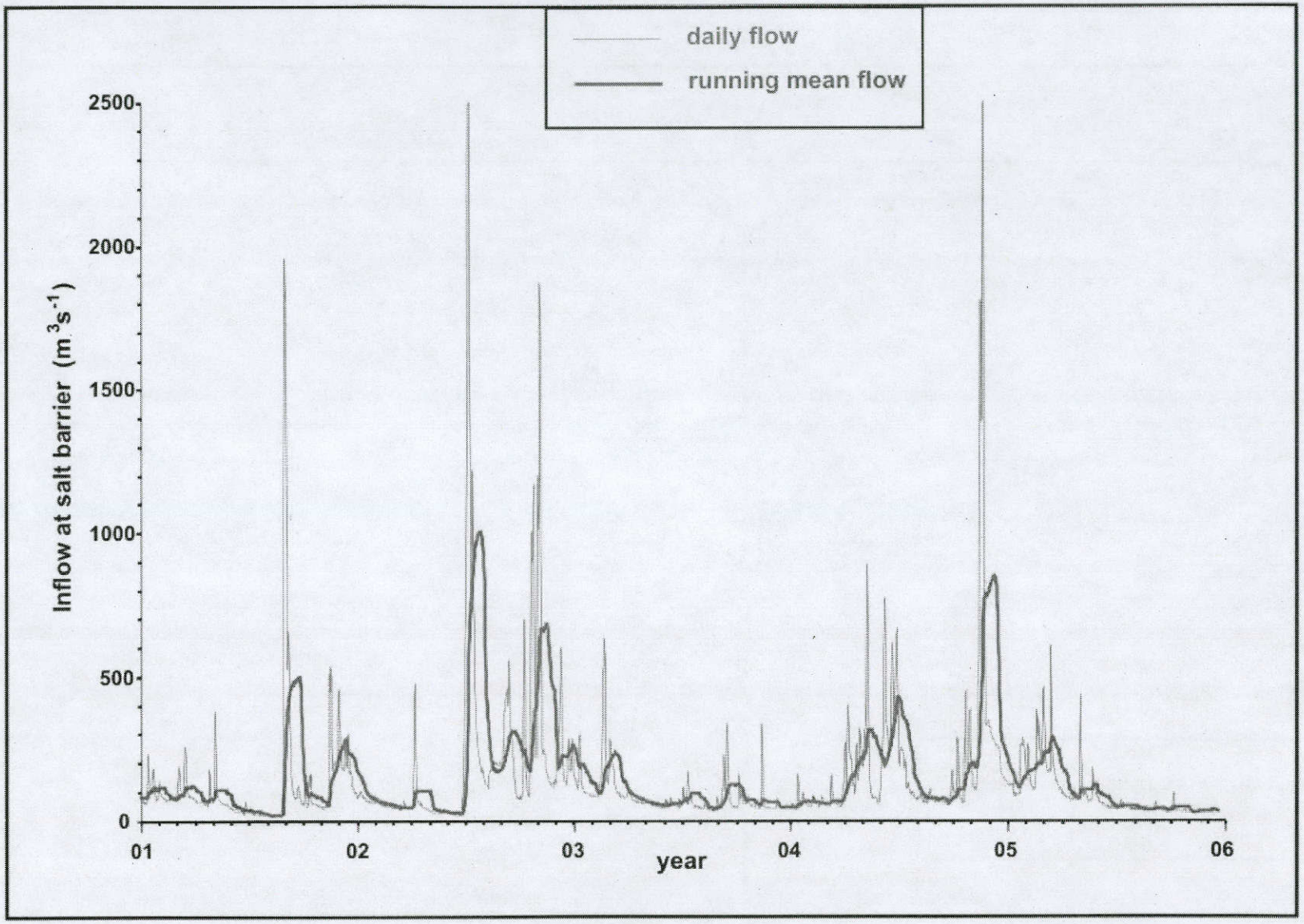

Figure 17(f) - Continued, 2001-05

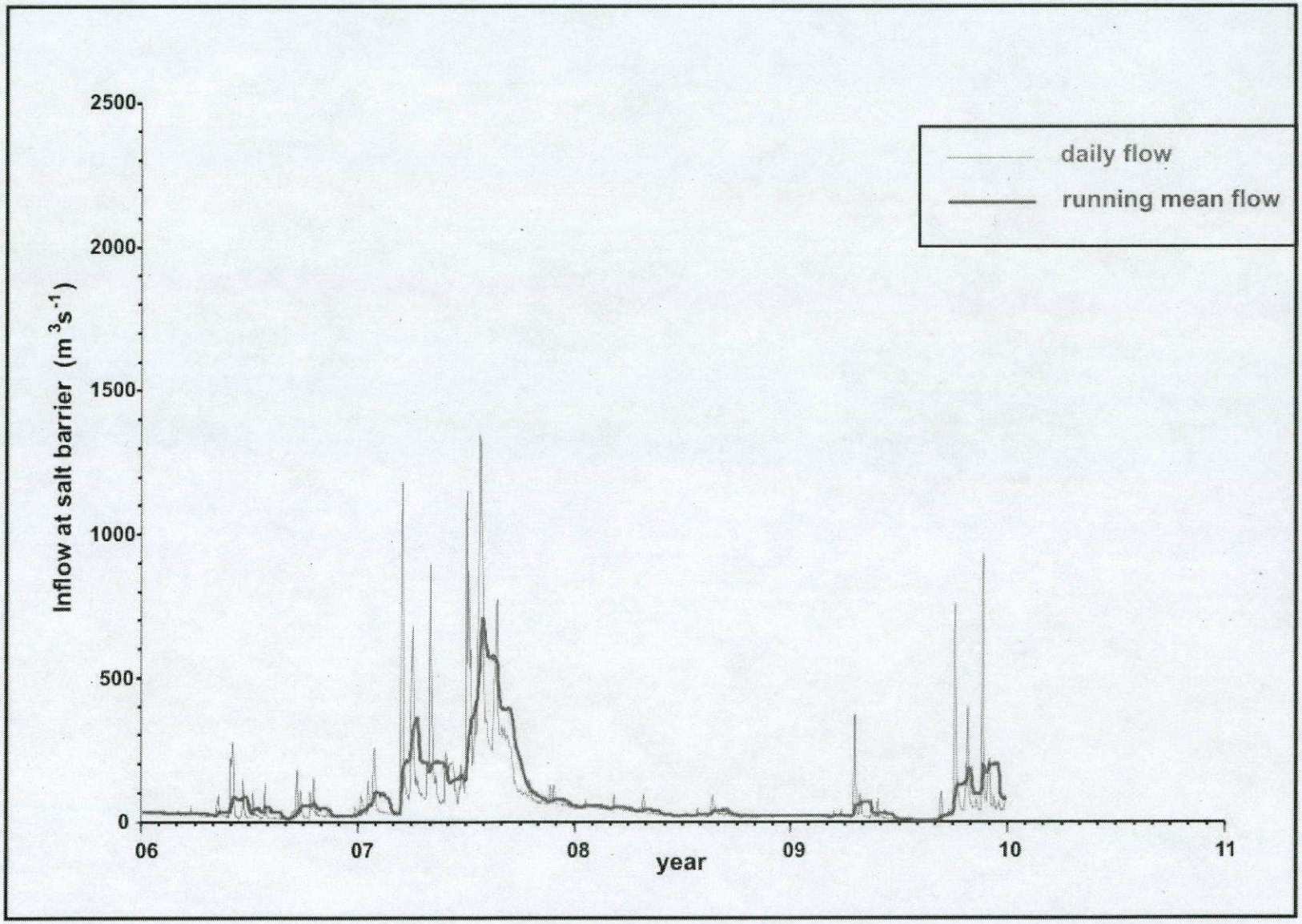

Figure 17(g) - Continued, 2006-11

3. STATISTICAL RELATION OF SALINITY IN SAN ANTONIO BAY TO INFLOW

In Chapter 1, the high variance of salinity in estuaries was remarked, a variance that is due to several factors other than streamflow, and which ultimately delimits the confidence in a one-to-one relation of salinity on inflow. Despite this high variance, the potential utility of a simple functional relation between salinity and inflow makes the formulation of such a relation the first step in an analysis of salinity behavior, not only for its predictive value, but also as a diagnostic basis for exploring the underlying mechanics. The statistical analysis is composed of three basic tasks: (1) compilation of a suitable data base of salinity measurements; (2) from a preliminary study of salinity variation, selection of a suitable functional form for the relation; (3) application of a fitting procedure, typically minimization of the squared variance, to determine the parameters of the relation, and quantification of its uncertainty.

3.1 Data sources

There are two classes of salinity data routinely acquired in the Texas estuaries: (1) point measurements at stations distributed in the estuary, and (2) time series of salinity at a fixed station determined by a robot monitor (an automatic "sonde"). Neither is entirely suitable. The point measurements (1) may have good spatial representation if they are scattered widely through the system, but they are typically sparse in time.

The usual practice of estuary hydrographers is to collect point measurements, usually from several monitoring programs, then group within subregions of the estuary. This is the procedure employed in both of the National Estuary Program projects on the Texas coast to analyze salinity trends in Galveston Bay and Corpus Christi Bay. The fact that they are measured at different locations within a subregion is a source of scatter additional to those enumerated above. In San Antonio Bay, salinity point data have been acquired from the Texas Commission on Environmental Quality, the Texas Department of Health, and Texas Parks and Wildlife Department. (There is a project underway at present to recover and digitize such data from past programs in San Antonio Bay. This data will be used to increase both the time-space density of

samples in the database of the present project, and to extend the period of record back in time, and will be reflected in future revisions of the present report.) San Antonio Bay was segmented into subregions for the analysis of salinity, as well as other relevant variables, as delineated in Fig.6. Accordingly, these data were sorted into the segments of Fig. 6. The primary limitation on these data is that prior to the digital record of TPWD, which begins in 1982 for this bay, the point measurements are so few that they are of no use in the present analysis. Total inflow data into San Antonio Bay ends in 2009, the last data available from operation of the TWDB TxRR model to determine the ungauged contribution (see Ward, 2010b). Thus, the period of analysis in the present study is 1982-2009.

The sonde measurements have good time continuity because of the high sampling rate, but are typically sparse in space. It would seem logical to incorporate such data into the compilation of point-measurement data. The high sampling rate of sondes (sometimes at intervals of one or two minutes) enables these devices to acquire data sets of thousands of measurements. This poses a problem, however, because salinity is highly autocorrelated, and measurements this close in time are typically redundant. In any statistical analysis, the sheer number of such data will dominate the results, a version of the pseudoreplication fallacy. In order to integrate sonde data into the point-measurement data base, it is necessary to subsample the sonde record to minimize redundance while exploiting the information in the record. For present purposes, one sonde was employed in this data base, the mooring at GBRA#1, supported by Guadalupe Blanco River Authority and San Antonio River Authority and operated by the Blucher Institute of Texas A&M – Corpus Christi. From the record of this sonde, measurements obtained daily at 1200 CST were extracted and incorporated into the data base for the Lower Bay segment.

The sonde records can be used as a concrete example of the variance in salinity in this system. Figure 18 displays a pair of two-year records showing the daily sonde measurements, and the daily inflow to the estuary (at the salt barrier) (cf. Fig. 17). While there is a general response of salinity to inflow surges, i.e., reducing salinity with increasing flow, the individual responses are inconsistent with the flow signal. Note especially the dramatic decreases in salinity in August and December of 2005, and in March and September of 2008, despite the sustained low flows. All of the processes summarized in Chapter 1, and quantified in Chapter 2, are at work to modify

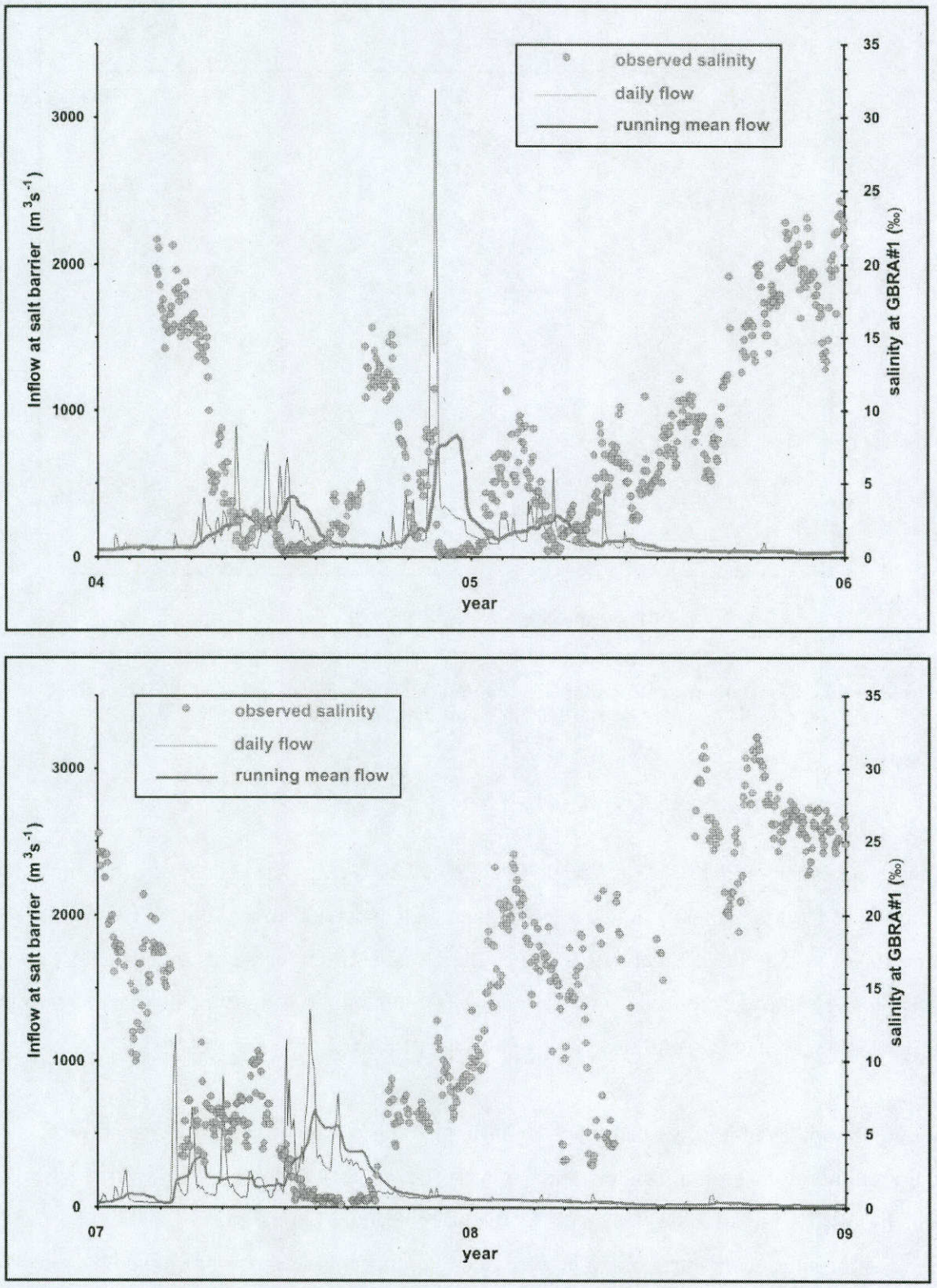

Figure 18 - Sonde-measured salinity at GBRA#1 with flow into San Antonio Bay at salt barrier, 2004-2005 (above) and 2007-2008 (below)

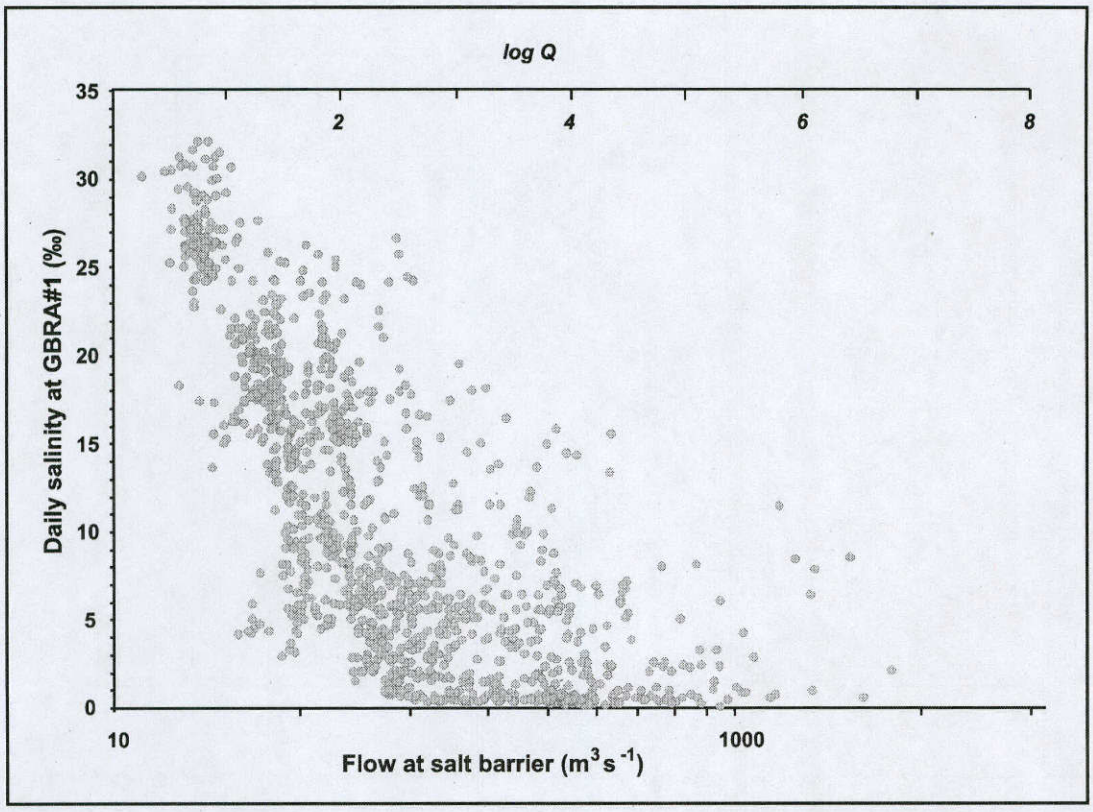

Figure 19 - Daily salinity at GBRA#1 versus natural logarithm of daily inflow at the salt barrier, 2004-05 and 2007-08 (same data as in Fig. 18)

salinity independent of the level of inflow. Even in late 2008 (Fig. 18) after steady low flows for over a year, the salinity signal continues to vacillate with excursions over 10 ppt. This is demonstrated by the plot of Figure 19, in which these same salinity data are plotted against the corresponding value of daily flow. (Actually, Fig. 19 plots salinity versus the naperian logarithm of flow to better spread the salinities in the mid-range of flows.)

Certainly the spikes of inflow hydrographs contribute to the scatter of salinity versus flow, because salinity does not immediately react to these sudden rises and falls in inflow, see especially April – July of 2004, January – March of 2005, and March – May of 2007 in Fig. 18. The use of the antecedent mean might be expected to reduce this scatter, since it would average the individual storm hydrographs. As shown in Figure 20, the variance is indeed reduced by this

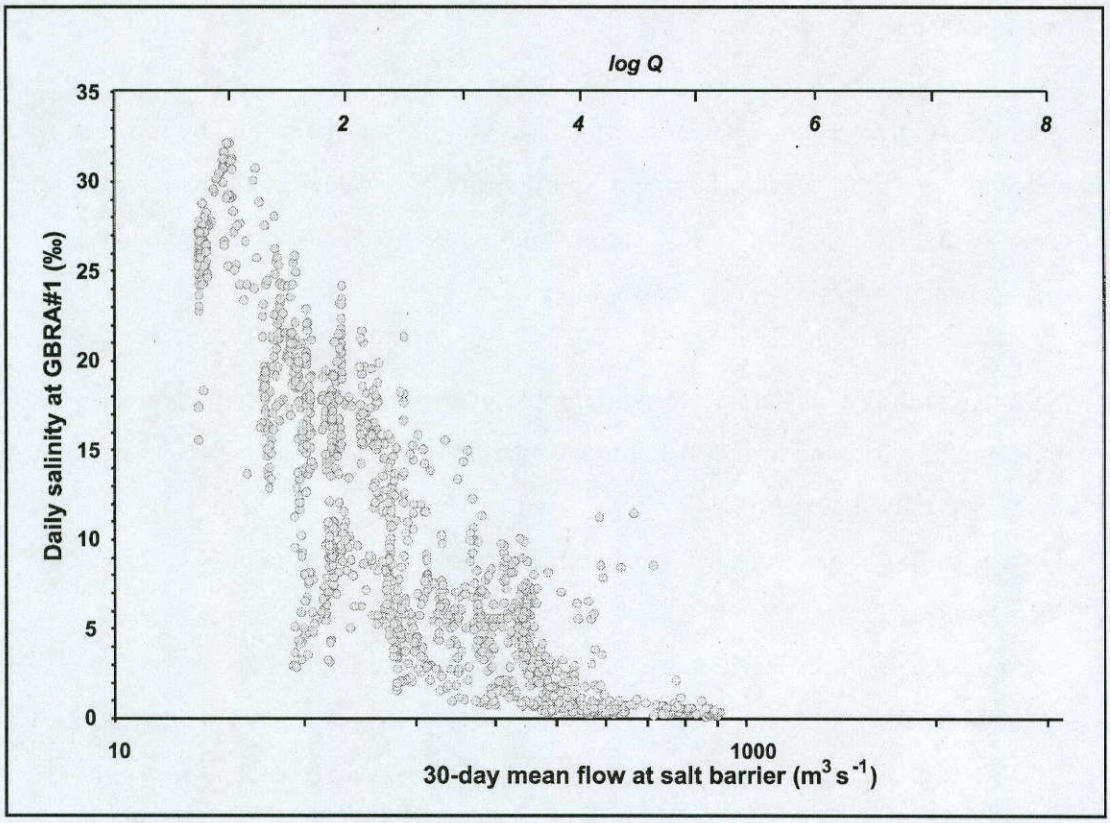

Figure 20 - Daily salinity at GBRA#1 versus natural logarithm of 30-day antecedent mean inflow at the salt barrier, 2004-05 and 2007-08 (same data as in Fig. 18)

device. The fact that long periods of sustained low flows in late 2005 and throughout 2008 render the daily and 30-day mean values virtually equal (Fig. 18), yet there is considerable variation in salinity, means that such averaging cannot reduce the contribution to variance in these time periods.

3.2 Regression forms

The objective is to extract as good a relation of salinity to inflow as permitted by the data, for use as an approximate predictor of salinity in San Antonio Bay. The above examination of a time signal of salinity at a specific point in Lower San Antonio Bay leads to some immediate conclusions about the form such a relation should take.

(1) Salinity exhibits considerable variation in San Antonio Bay, much of which is unrelated to flow, and is a probably manifestation of the other processes addressed in Chapters 1 and 3.
(2) Despite the high scatter, there is a general trend for decreasing salinity with increasing flows.
(3) The mid-range salinity relation to flow is better depicted with logarithm of flow as the independent variable.
(4) The high variance in this relation deriving from the rise and recession of storm hydrographs, to which salinity, especially in the lower bay, does not immediately respond, can be mitigated by an antecedent averaging of flow.

Because the present objective is a focus on the long-term salinity responses, some additional mitigation of salinity variance arising from factors other than inflow could be achieved by averaging the measured salinities. For this purpose, the salinity data, already aggregated over the spatial area of the segment (Fig. 6), were averaged by month. The associated inflow data to be paired with these averaged salinity values were the 30-day antecedent mean flow at the end of each month. Even considering flows and salinities with a monthly time resolution, there is still a memory effect, in which salinity exhibits a lagged, integrated response to inflows. This can be captured to some extent by averaging the inflows over several months, preceding and including the month for which mean salinities are available, in the same way that use of an averaged inflow in Fig. 20 reduced the variance of the relation from that of Fig. 19. Numerical experiments with the 1982-2009 data disclosed that a four-month average inflow (i.e., the mean of the present and the preceding three months) achieved the greatest explained variance of the predicted monthly

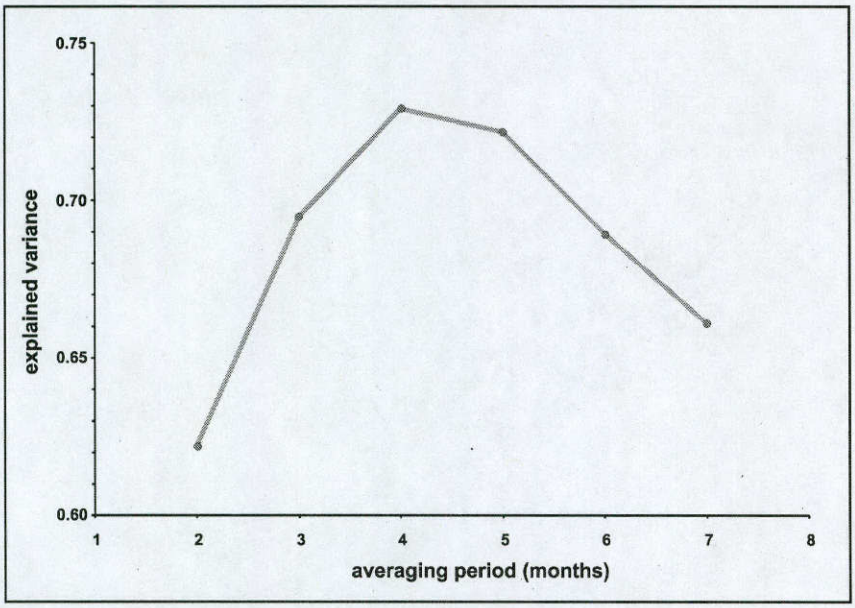

Figure 21 - Explained variance (linear) of monthly mean salinity versus inflow at salt barrier averaged over multiple months

salinity, see Figure 21. The monthly salinity data for the Lower Bay segment are plotted versus the four-month mean flows in Figure 22. Data points are differentiated as those before the GBRA-1 sonde became operational (i.e., before March 2004), and those afterward. The former averaged about 5 data points per month and the latter about 33, but there is no obvious bias between the two.

Selection of a regression form is based upon qualitative information about the observed behavior of the dependent variable on the independent. A linear regression is the obvious first choice,

$$S = a + b \log Q$$

and behaves satisfactorily for the midrange of salinities (which is the majority of the data). The best-fit linear regression is plotted in Fig. 22. However, a linear regression has an undesirable property of not being able to represent the nonlinear behavior of salinity at high and low flows:

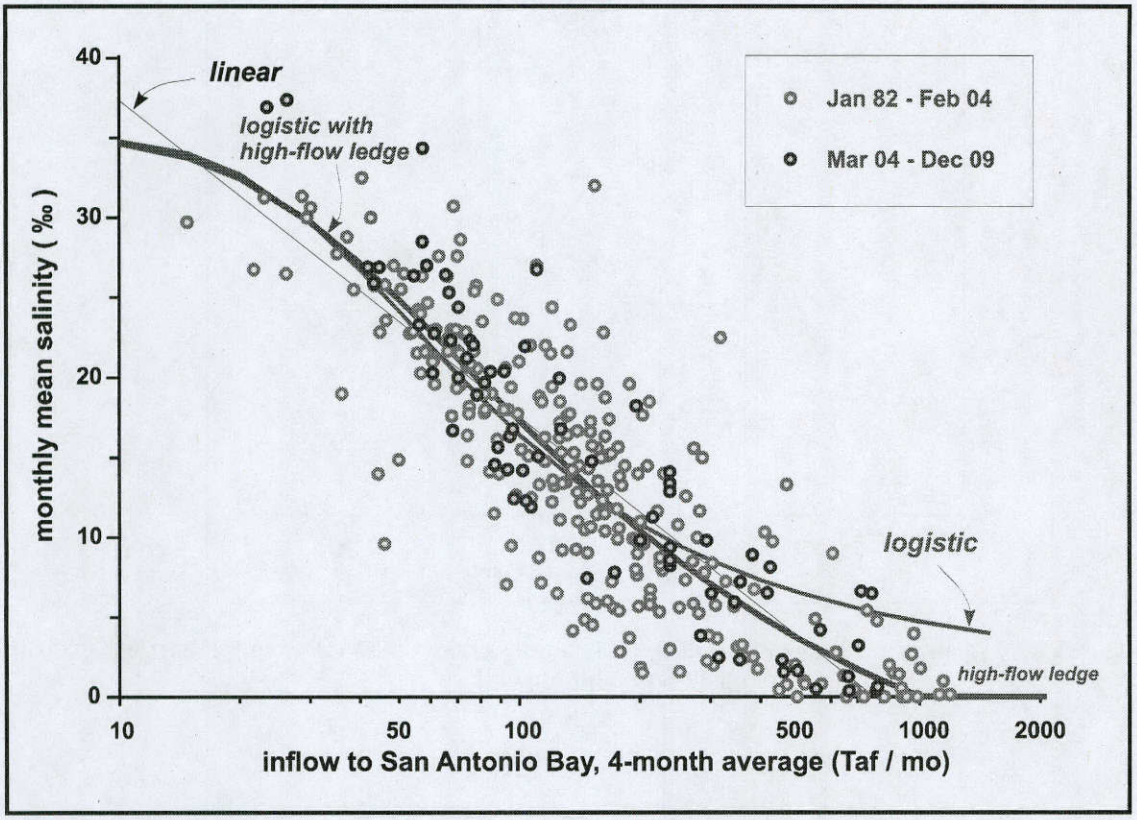

Figure 22 - Monthly-mean salinity in Lower Bay (Fig. 6) versus inflow into San Antonio Bay averaged over four months terminating with the month of salinity data, with regression lines (see Table 1)

indeed the linear relation predicts salinities substantially above seawater for very low flows and negative salinities for high flows. A better physical representation of the variation of salinity with flow is a sigmoid shape, in which the dependent variable approaches asymptotes at high and low values of the independent variable. We know that sufficiently high flows drive the salinity to zero, which defines the lower asymptote, and for low flows the salinity approaches seawater, which defines the upper asymptote. Actually, with distance south along the Texas coast, the evaporative deficit at the surface increases, so that under low flows, especially in summer, salinities can exceed seawater. (If we had more data at very low flows, it might have been possible to improve the specification of the upper asymptote, perhaps increasing it by a few parts per thousand.)

Table 4 - Regressions of monthly salinity versus inflows for Lower Bay (Fig. 6)

regression	*equation*	*Expl var (%)*	*SEE (ppt)*
(1) linear	$S = 57.15 - 8.598 * log(Q)$	72.7	4.5
(2) logistic	$S = 35\ [1 + exp\{-24(1/logQ - 1/log90)\}]^{-1}$	71.6	4.6
(3) logistic with high-flow ledge	$S = max\{35\ [1 + exp\{-20(1/logQ - 1/log210)\}]^{-1} - 15, 0\}$	74.4	4.4

where:

S = monthly-mean Lower Bay salinity in ppt (‰)
Q = total inflow into San Antonio Bay in thousands of acre feet (Taf) per month, present month averaged with preceding three (3) months (see text)
Expl var = explained variance of the regression (for the linear regression this equals R^2)
SEE = standard error of the estimate
log denotes the Naperian logarithm

There are a number of sigmoid functions on the market. For this work, a logistic function was selected.

$$S = \frac{C}{1 + Ae^{-B \log Q}}$$

(The arctangent and the Gaussian error function were also tried, but proved essentially equivalent to the logistic.) A least-squares fit of the logistic to the salinity-inflow data was carried out iteratively (see, e.g., Cavallini, 1993), plotted in Fig. 7. A slightly more complicated version is a sigmoid with a ledge on either asymptote: in this case, a high-flow ledge was used to improve the functional behavior at low salinities. All three best-fit regressions for the Lower Bay segment are shown in Table 4 above.

All of these regressions achieve better than 70% explained variance, the logistic with high-flow shelf performing best. Even though the explained variance of the simple logistic is slightly

poorer than the linear, it performs in a more physical realistic manner at high and low values of flow. Table 4 also tabulates the uncertainties of each, as a standard error. Basically, these uncertainties are virtually identical, about 4 ‰. This means that the 95% confidence band of these three regressions is ± 8 ‰, a sober measure of the intrinsic variability of salinity, even with the averaging of both salinity and inflow implicit in these regressions.

References

Cartwright, D. E., 1999: *Tides: a scientific history.* Cambridge: University Press.

Cavallini, F., 1993: Fitting a logistic curve to data. *College Mathematics Journal 24* (3), pp 247-253.

Doodson, A. T., 1928: The analysis of tidal observations. Phil. Trans. Roy. Soc. Lond. 227, 223-279.

Dyke, P., 2007: *Modeling coastal and offshore processes.* London: Imperial College Press.

Guadalupe-San Antonio Bay and Basin Expert Science Team, 2011: Environmental Flows Recommendations Report. Texas Commission on Environmental Quality, Austin. http://www.tceq.texas.gov/permitting/water_rights/eflows/guadalupe-sanantonio-bbsc

Guthrie, C.G., 2010a: TxBLEND model calibration and validation for the Guadalupe and Mission-Aransas Estuaries. Austin: Bays and Estuaries Program, Texas Water Development Board.

Guthrie, C.G., 2010b: TxBLEND model validation for the Upper Guadalupe Estuary using recently updated inflow data. Austin: Bays and Estuaries Program, Texas Water Development Board.

Hearn, C.J., 2008: *The dynamics of coastal models.* Cambridge, U.K.: Cambridge University Press.

Longley, W.L. (ed.), 1994: *Freshwater inflows to Texas bays and estuaries: Ecological relationships and methods for determination of needs.* Austin: Texas Water Development Board and Texas Parks & Wildlife Department.

Mangelsdorf, P. C., 1967: Salinity measurements in estuaries. In: *Estuaries* (G. Lauff, ed.), AAAS Publ. 83, 1340-1357. Washington, D.C.: American Association for the Advancement of Science.

Nash, J., and J. Sutcliffe, 1970: River flow forecasting through conceptual models: Part I, A discussion of principles. *J. Hydrol. 10*, pp 282-290.

Pugh, D. T., 1987: *Tides, surges and mean sea-level.* Chichester: John Wiley & Sons.

Ward, G.H., 1982: Pass Cavallo, Texas: Case study of tidal-prism capture. *J. Waterway, Port, Coastal & Ocean Div., Proc. Am. Soc. Civil Engrs. 108* (WW4).

Ward, G.H., 1993: The prediction problem for salinity. *Proceedings, Second State of the Bay Symposium* (R. Jensen, R. Kiesling, F. Shipley, eds.), Report GBNEP-23, Galveston Bay National Estuary Program, Webster, Texas.

Ward, G. H., 1997: *Processes and trends of circulation within the Corpus Christi Bay National Estuary Program study area.* Report CCBNEP-21, Corpus Christi Bay National Estuary Program, Corpus Christi.

Ward, G.H., 2004: Texas water at the century's turn—perspectives, reflections and a comfort bag. Chapter 2 in: *Water for Texas* (J. Norwine, J. Giardino & S. Krishnamurthy, eds.), pp. 17-43. College Station: Texas A&M University Press.

Ward, G. H., 2010a: *A timeline of Cedar Bayou.* TWDB Interagency Contract 0900010973, Center for Research in Water Resources, University of Texas at Austin.

Ward, G.H., 2010b: *Inflows to San Antonio Bay.* TWDB Interagency Contract 0900010973, Center for Research in Water Resources, University of Texas at Austin.

Ward, G.H., 2011: Water resources and water supply. Chap. 3 in: *The impact of global warming on Texas* (J. Schmandt, G. North and J. Clarkson, eds.). Austin: The University of Texas Press.

Ward, G. H., 2012: *The blue crab: a survey with application to San Antonio Bay.* TWDB Interagency Contract 0900010973, Center for Research in Water Resources, University of Texas at Austin.

Ward, G. H., and N.E. Armstrong, 1992: *Ambient Water and Sediment Quality of Galveston Bay: Present Status and Historical Trends.* Report GBNEP-22 (4 vols.). Webster, Texas: Galveston Bay National Estuary Program.

Ward, G., and C. Montague, 1996: Estuaries. Chapter 12 in *Water Resources Handbook* (L. Mays, ed.), 12.1 - 12.114. New York: McGraw-Hill Book Company.